THERMOPHORESIS AND BROWNIAN MOTION EFFECTS ON INCLINED MHD NANO-FLUID FLOW WITH MULTI SLIP CONDITION

Gopal Nanda[1], Harshad Patel[1*]

[1] Gujarat Technological University, Ahmedabad, Gujarat, India
[1*]U V Patel College of Engineering, Ganpat University, Mehsana, Gujarat, India
Corresponding Author: Harshad Patel [1*]
Email: [1*]harshadpatel2@gmail.com,

Abstract

The current study focuses on the analysis of free convection flow of MHD Nano-fluid in the presence of magnetic fields. Various physical parameters such as thermal radiation, thermophoresis, Brownian motion, chemical reaction, and gyrotactic micro motile organisms are taken into account on a continuous stretching of a two-dimensional sheet. The governing equations are formulated as systems of PDEs, which are then transformed into a dimensionless system of ODEs using similarity transformation. The appropriate HAM method is utilized to solve the governing problems and the results for velocity, temperature, concentration, and Micro Organism profiles are obtained. The impacts of different physical parameters are illustrated through graphs. The numerical values for Skin friction, Temperature gradient, Concentration gradient, and Micro motile number are presented in tabular form. The findings indicate that the inclination parameter and Magnetic field parameter tend to decrease the fluid motion, while the heat transfer process enhances with thermophoresis and Brownian motion. This study has significant implications in various fields such as heat control systems, food factories, thermal exchangers, biomechanics, biomedical engineering, and aero dynamical systems.

Keywords: Nano-fluid; MHD; Brownian motion; Thermophoresis; HAM

NOMENCLATURE

B_0 Magnetic field	R Radiation
u Velocity profiles in x direction	Nr Buoyancy ration value
v Velocity profiles in y direction	σ Electrical conductivity
G_t local thermal Grashoof number	β_T Thermal expansion (Volumetric coefficient)
ρ density	R_b Bio convective Reyligh number
μ Dynamic viscosity	Nb Brownian motion parameter
g Acceleration due to gravity	Nt Thermophoresis parameter
ν Kinematic viscosity	S_f hydrodynamic Slip
S_t Thermal Slip	S_p Solutal Slip
Gr Thermal Grashof number	η Similarity variable
S_g Nano-particle slip	P_e Peclet number

Sc Schmidt number	M Magnetic parameter
T Fluid temperature	D_T Thermophoresis diffusion coefficients
Pr Prandtl number	L_b Lewis number
C_p Specific heat at constant pressure	C Concentration
θ Dimensionless fluid temperature	D_B Brownian motion

1. INTRODUCTION

One of the primary requirements in various industrial technologies is the need for ultrahigh-performance cooling. However, a major limitation in achieving this is the inherently low thermal conductivity of energy-efficient heat exchanger fluids. Advanced technology has enabled the production of metallic or non-metallic particles at nanometer dimensions. Nanoparticles exhibit unique electrical, mechanical, and thermal properties. Nanofluids are formed by suspending nano solid particles, typically ranging in size from 1 to 100 nm, in conventional fluids such as ethylene glycol, water, and oil. Research conducted by Choi and Eastman [1-2] has demonstrated that dispersing nanoparticles enhances the heat transfer capabilities of water. Imran et al. [3] explored the impact of electrically conducting mixed convection flow of Casson nanofluid created by a moving wedge in the presence of thermal radiation. Sheikholeslami et al. [4] investigated the unsteady nanofluid flow between parallel plates using the Differential Transformation Method, considering factors such as the radiation parameter, squeeze number, Hartmann number, Brownian motion parameter, and thermophoretic parameter on temperature and concentration profiles. Hayat et al. [5] analyzed the magnetohydrodynamic stagnation point flow of Carreau nanofluid towards a stretching sheet in the presence of thermal radiation and chemical reaction. Habib and Amir [6] studied the impact of nanoparticles on fluid flow between parallel plates filled with porous media in the presence of magnetic fluid.

Magnetohydrodynamics is concerned with the behavior of fluids that possess significant electrical conductivity and interact with a magnetic field. When an electrically conducting fluid moves in the presence of a magnetic field, electric currents are induced within the fluid. The impact of magnetohydrodynamics extends to various fields such as electromagnetic costs, hydraulic systems, astrophysical phenomena, blood circulation in the human body, transformation of liquid into metal, plasma confinement, and a range of social and environmental issues. Hartman [7] has specifically investigated laminar flow in the presence of a magnetic field. Babu et al. [8] have explored the influence of thermal and solutal Grashof numbers on two-dimensional flow, as well as the characteristics of heat and mass transfer in magnetohydrodynamic flow with thermophoresis and Brownian motion effects. Mabood et al. [9] have studied the impact of viscous dissipation and heat source on chemically radiative magnetohydrodynamic boundary layer flow of a nanofluid past a rotating stretching sheet. Kataria and Mittal [10] have focused on the hydromagnetic gravity-driven convective boundary layer flow of nanofluids past an oscillating vertical plate in the presence of a uniform transverse magnetic field and thermal radiation. Sheikholeslami et al. [11] have examined the effects of thermal diffusion and heat generation on the unsteady magnetohydrodynamic flow of radiating and electrically conducting nanofluid past an oscillating vertical plate through a porous medium. Patel et al. [12] have analyzed the combined impact of thermal radiation and non-uniform heat generation and absorption on the unsteady magnetohydrodynamic flow of a micropolar fluid due to a non-linear stretched sheet in a porous medium. Kataria and Patel [13] have discussed the effects of parabolic motion, thermo-diffusion, heat generation/absorption, thermal radiation, and chemical reaction on free convective unsteady magnetohydrodynamic second-grade fluid flow near an infinite vertical plate through a porous medium.

The inclusion of thermal radiation in fluid flow presents numerous challenges and has a significant impact on heat transfer rates. Thermal radiation finds valuable applications in solar technology, the aeronautics industry, and spacecraft activities. The pioneering work on thermal radiation was conducted by Rosseland [14]. Sulochana [15] examined the impact of transpiration on the flow of a Carreau nanofluid near a stagnation-point toward a stretching/shrinking sheet in the presence of Brownian motion and thermophoresis effects. Iskandar [16] sought to expand the exploration of the unique characteristics of the Reiner–Philippoff fluid by incorporating Brownian and thermophoresis diffusion with MHD circumstances and radiative heat transfer. Kalpana et al. [17] explored the characteristics of magnetohydrodynamics hybrid nanofluid flow in an irregular wall, incorporating the effects of Brownian motion and thermophoresis. Hatami and Ghasemi [18] examined the complete conditions, including the four important forces acting on nanoparticles in a porous medium, namely gravity, drag, thermophoresis, and Brownian forces, to obtain physical and realistic results. Tawade et al. [19] studied the effects of thermophoresis and Brownian motion on temperature and concentration for boundary layer flow of a Casson nanofluid over a linearly stretched sheet. Shahzad et al. [20] explored the effects of temperature-dependent properties on non-Newtonian flow over an inclined surface in the presence of chemical reaction, Brownian motion, thermophoresis, and viscous dissipation. Cao et al. [21] simulated and investigated the free convection of Cu-water nanofluid inside a square heat exchanger chamber in the presence of an MHD magnetic field. Mehdi [22] studied the importance of thermophoresis in particle distribution and obtained concentration distribution considering thermophoresis along with the effects of the other three factors mentioned above. Mittal and Kataria [23] examined the influence of radiation on the flow of three-dimensional CuO-water nanofluid between two horizontal parallel plates in a rotating system through a porous medium.

In the realm of literature, there has been a noticeable lack of emphasis on the significance of MHD nanofluid with slip and without slip conditions in the presence of nonlinear thermal radiations, motile microorganisms, and chemical reactions. Our current study delves into the impact of slip and without slip conditions in conjunction with Brownian motion, chemical reactions, radiation, motile microorganisms, inclined MHD, and thermophoresis effects on MHD nanofluid dynamics within a two-dimensional fluid flow. The resulting governing differential equations exhibit nonlinearity, and through a practical similarity transformation, the partial differential equations are converted into ordinary differential equations. These nonlinear governing equations were subsequently solved numerically using MATHEMATICA, with the results being presented in both tabular and graphical formats. The analysis includes discussions on different parameters concerning velocity, temperature, concentration, and micro motile profiles. The insights and observations outlined in this study have the potential to enhance our comprehension of inclined MHD nanofluid flow.

2. MATHEMATICAL FORMULATION

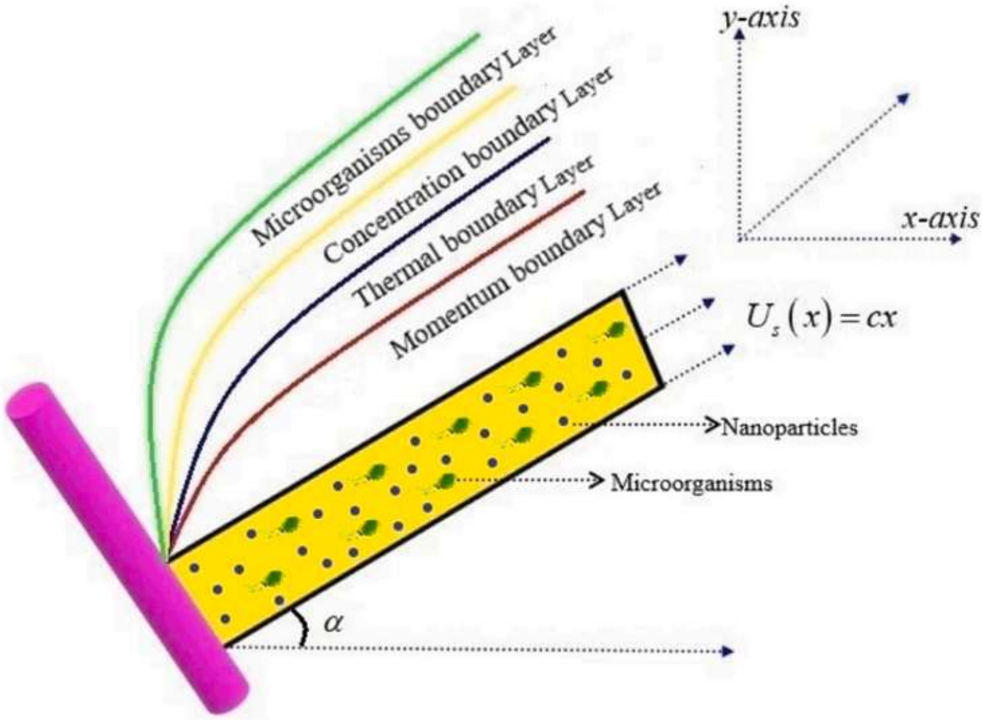

Figure 1: Physical sketch of the problem

Consider the steady of MHD Nano-fluid flow with magnetic field effects in continuous stretching two-dimensional non-linear stretching sheet. The sheet is extended across the fluid flow with the fixed origin given the impact of opposing forces. The flow is considered as incompressible laminar flow. The base fluid to be considered as water and iron oxides are taken as nanoparticles. The geometry of the flow which is shown in Figure 1. The coordinate system to be chosen as x-axis along the surface whereas, y-axis consider perpendicular to it which is describe in Figure 1 and the flow is confine with $y > 0$. The B_0 (magnetic field) is applied in y-axis direction. There is a nonuniform velocity $U(x,t) = \frac{ax}{1-\lambda t}$ along the x-axis of the sheet. The temperature adjusted T_f and concentration is assumed C_w at the surface. The ambient temperature T_∞ and ambient concentration C_∞ is considered at $y \to \infty$. The induced magnetic field and electrical field. Under above assumption, the governing velocity, heat transfer, mass transfer and Micro Organism equations can be express as,

$$\frac{\partial u}{\partial x} + \frac{\partial u}{\partial y} = 0 \quad (1)$$

$$\left(u\frac{\partial u}{\partial x} + v\frac{\partial v}{\partial y}\right) = (v)\left(\frac{\partial^2 u}{\partial y^2}\right) - \frac{v}{K}u - \frac{\sigma B_0^2 \sin\alpha}{\rho}u + \frac{g}{\rho_f}(1 - C_\infty)\,\rho f_\infty(\beta)_{nf}(T - T_\infty) - (\rho_p - \rho f_\infty)(C - C_\infty)(N - N_\infty) \quad (2)$$

$$u\frac{\partial T}{\partial x} + v\frac{\partial T}{\partial y} = \frac{k}{\rho c_p}\frac{\partial^2 T}{\partial y^2} - \frac{1}{\rho c_p}\frac{\partial q_r}{\partial y} + \tau\left(D_B\frac{\partial C}{\partial y}\frac{\partial T}{\partial y} + \frac{D_T}{T_\infty}\left(\frac{\partial T}{\partial y}\right)^2\right) \quad (3)$$

$$u\frac{\partial C}{\partial x} + v\frac{\partial C}{\partial y} = D_B\frac{\partial^2 C}{\partial y^2} + \frac{D_T}{T_\infty}\frac{\partial^2 T}{\partial y^2} \quad (4)$$

$$u\frac{\partial N}{\partial x} + v\frac{\partial N}{\partial y} + \frac{bW_c}{(C_w - C_\infty)}\left[\frac{\partial}{\partial y}(NC_y)\right] = D_B\frac{\partial^2 N}{\partial y^2} \quad (5)$$

$u = U(x,t) + U_{slip}, v = v_w, T = T(x,t) + T_{slip}, C = C(x,t) + C_{slip}, N = N(x,t) + N_{slip} \ \ at\ y = 0.$ (6)

$u \to 0, v \to 0, T \to T_\infty,\ \ C \to C_\infty, N \to N_\infty;\ as\ \ y \to \infty$ (7)

The radiation heat flux can be express as [24],

$$q_r = -\frac{4\sigma^*}{3k^*}\frac{\partial T^4}{\partial y}. \quad (8)$$

Expansion of T^4 using Taylor series at T_∞ and higher order terms neglecting,

$$T^4 \cong 4T_\infty^3 T - 3T_\infty^4 \quad (9)$$

Substituting values of equation (15) in (14),

$$q_r = -\frac{4\sigma^*}{3k^*}\frac{\partial\left(4T_\infty^3 T - 3T_\infty^4\right)}{\partial y} \quad (10)$$

After differentiation of equation (16) with respect of y and substituting in equation (4),

$$u\frac{\partial T}{\partial x} + v\frac{\partial T}{\partial y} = \frac{k}{\rho c_p}\frac{\partial^2 T}{\partial y^2} - \frac{1}{\rho c_p}\frac{16\sigma^* {T_\infty^3}^3}{3k^*}\frac{\partial^2 T}{\partial y^2} + \tau\left(D_B\frac{\partial C}{\partial y}\frac{\partial T}{\partial y} + \frac{D_T}{T_\infty}\left(\frac{\partial T}{\partial y}\right)^2\right) \quad (11)$$

The dimensionless variable is introducing,

$$\eta = \sqrt{\frac{a}{\nu}}y, u = axf'(\eta), v = ax,\ \chi(\eta)(N_w - N_\infty) = N - N_\infty, w = -\sqrt{(a\nu)} \quad (12)$$

Therefore, the governing equations in dimensionless form are as follows,

$$F''' + F''F - {F'}^2 - M^2F' + Gr(\theta - N_rC - R_bN) = 0 \quad (13)$$

$$\frac{(1+R)}{Pr}\theta'' + \theta'F - F'\theta + NbC'\theta' + Nt{\theta'}^2 = 0 \quad (14)$$

$$C'' + Sc\,(FC') + \frac{Nt}{Nb}\theta'' = 0 \quad (15)$$

$$\chi'' + \Pr L_b\,\chi' - P_e(C''(\sigma + \chi) + \chi'C') = 0 \quad (16)$$

Subject to

$$F(\eta) = f_w, F'(\eta) = 1 + S_f\,F''(\eta), \theta(\eta) = 1 + S_t\theta'(\eta), C(\eta) = 1 + S_pC'(\eta), N(\eta) = 1 + S_gN'(\eta)\ \ at\ \eta = 0 \quad (17)$$

$$F'(\eta) \to 0, G(\eta) \to 0, \theta(\eta) \to 0, C(\eta) \to 0\ at\ \eta \to \infty \quad (18)$$

$$M^2 = \frac{\sigma {B_0}^2 \sin\alpha}{\rho}, Pr = \frac{\nu}{\alpha}, Gt = \frac{\rho g \beta_T(T_w - T_\infty)}{\nu^2}x^3, R_e = \frac{U\,x}{\nu}, Gr = \frac{Gt}{{R_e}^2}, Sc = \frac{\nu}{D_B}, Nb = \frac{\tau D_B(C_w - C_\infty)}{\nu}, N_t = \frac{(T_f - T_\infty)\tau D_T}{\nu T_\infty}, R = \frac{16\sigma^*}{3k^*}\frac{{T^3}_\infty}{k_f}, N_r = \frac{\rho_p - \rho_f(C_w - C_f)}{\rho_f\beta(1 - C_\infty)(T_w - T_\infty)}, R_b = \frac{\rho_p - \rho_f(N_w - N_f)}{\rho_f\beta(1 - C_\infty)(T_w - T_\infty)}, P_e = \frac{bW_c}{D_B}$$

3. HAM SOLUTION

The modified homotopy analysis approach (HAM) proposed by Liao [25] is used to solve above ODEs equations along with the initial and boundary conditions. The auxiliary parameter $\hbar$ in our solution series gives us a simple and efficient way to modify and regulate the convergence of the series solution, also known as the $\hbar-$curve. The permissible region of this $\hbar-$curve is the horizontal line segment, and the $\hbar-$curves are plotted to determine the range in which these values are acceptable. In this case, auxiliary linear operators and an initial guess are needed for the HAM solution, which are shown below.

The set of initial guesses are:

$$F_0(\eta) = f_w + \left(\frac{1}{1+S_f}\right)(1-e^{-\eta}), \theta_0(\eta) = \frac{1}{1+S_t},\ C_0(\eta) = \frac{1}{1+S_p},\ \chi_0(\eta) = \frac{1}{1+S_g} \quad (19)$$

The set of linear operators are:

$$L_F = \frac{\partial^3 F}{\partial \eta^3} - \frac{\partial F}{\partial \eta}, L_\theta = \frac{\partial^2 \theta}{\partial \eta^2} - \theta, L_C = \frac{\partial^2 C}{\partial \eta^2} - C,\ \ L_\chi = \frac{\partial^2 \chi}{\partial \eta^2} - \chi \quad (20)$$

Which are satisfying the below given equations.

$$L_F(a_1 + a_2 e^{\eta} + a_3 e^{-\eta}) = 0 \quad (21)$$

$$L_\theta(a_4 e^{\eta} + a_5 e^{-\eta}) = 0 \quad (22)$$

$$L_c(a_6 e^{\eta} + a_7 e^{-\eta}) = 0 \quad (23)$$

$$L_\chi(a_8 e^{\eta} + a_9 e^{-\eta}) = 0 \quad (24)$$

Where $a_1, a_2, a_3, a_{4,} a_5, a_6, a_7, a_8, a_9$ are the playing a role of arbitrary constants.

3.1 NUMERICAL SOLUTION

To gain a deeper insight into how various physical parameters impact velocity, temperature, and concentration profiles was acquired through numerically with the utilization of the HAM toolbox within the Mathematica software.

3.2 SKIN-FRICTION, SHERWOOD NUMBER & NUSSELT NUMBER

Skin friction coefficient, Nusetl number, Sherwood number, and Micro motile density number, are defined by many researchers, like, Begum et al. [26], Pal and Mondal [27] and Ahmad et al. [28].

$$C_{F_x} = \frac{\tau_w}{\rho {U_w}^2} \quad (25)$$

$$N_{u_x} = \frac{x q_w}{k(T_w - T_\infty)} \quad (26)$$

$$S_{h_x} = \frac{x q_m}{D(C_m - C_\infty)} \quad (27)$$

$$\chi_{n_x} = \frac{x q_n}{D_m(N_w - N_\infty)} \quad (28)$$

Where, τ_w, q_w, q_m and q_n is the values of Shear stress, Local heat flux, Local mass flux and micro motile flux respectively, which is defined as,

$$\tau_w = \mu \frac{\partial u}{\partial y}\bigg|_{y=0} \quad (29)$$

$$q_w = -k \frac{\partial T}{\partial y}\bigg|_{y=0} \quad (30)$$

$$q_m = -D \frac{\partial C}{\partial y}\bigg|_{y=0} \quad (31)$$

$$q_n = -D_m \frac{\partial N}{\partial y}\bigg|_{y=0} \tag{32}$$

The dimensionless Nusselt number, Micro motile number, Skin-friction, and Sherwood number are written as under.

$$Re_{x^{1/2}} C_{F_x} = F''(0) \tag{33}$$

$$Re_{x^{-1/2}} N_{u_x} = \theta'(0) \tag{34}$$

$$Re_{x^{-1/2}} S_{h_x} = C'(0) \tag{35}$$

$$Re_{x^{-1/2}} N_{n_x} = \chi'(0) \tag{36}$$

Where, the local Reynolds numbers is $Re_x = u_w \frac{x}{\nu}$

3.3 CONVERGENCE ANALYSIS OF HAM SOLUTIONS

To find the range of auxiliary parameter namely h_F, h_θ, h_C and h_χ for convergence of solutions, corresponding $\hbar-$curves are plotted in Fig. (2). From these curves, it is seen that the acceptable ranges of aforesaid $\hbar-$curves are $-0.8 \le h_F \le 0.5, -0.8 \le h_\theta \le 0.5, -0.8 \le h_C \le 0.5$ and $-0.8 \le h_\chi \le 0.5$.

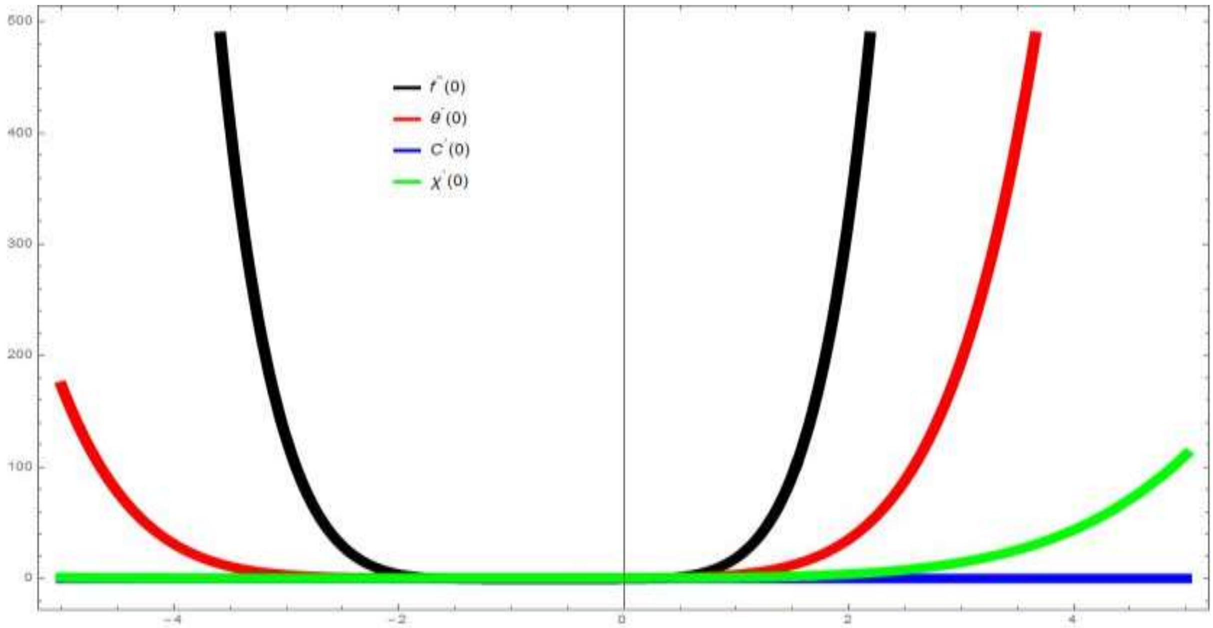

Fig. 2: h-curve

4. RESULTS AND DISCUSSION

This portion of the study delves into the findings and efficiency of the current research on the concentration profiles, motile microorganisms' profiles, temperature profiles, and velocity profile with respect to the parameters $M, Gr, Nr, Rb, R, Nb, Nt, Lb, Pe, \sigma$.

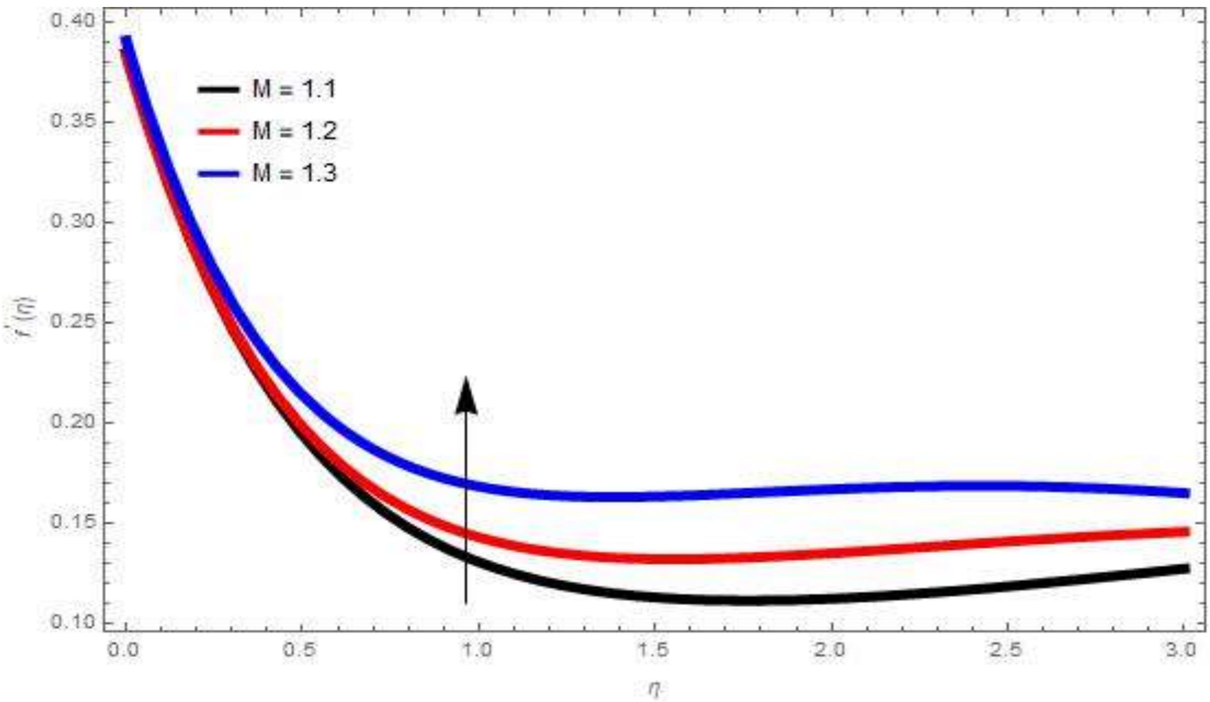

Fig. 3: M on $f'(\eta)$ with slip condition

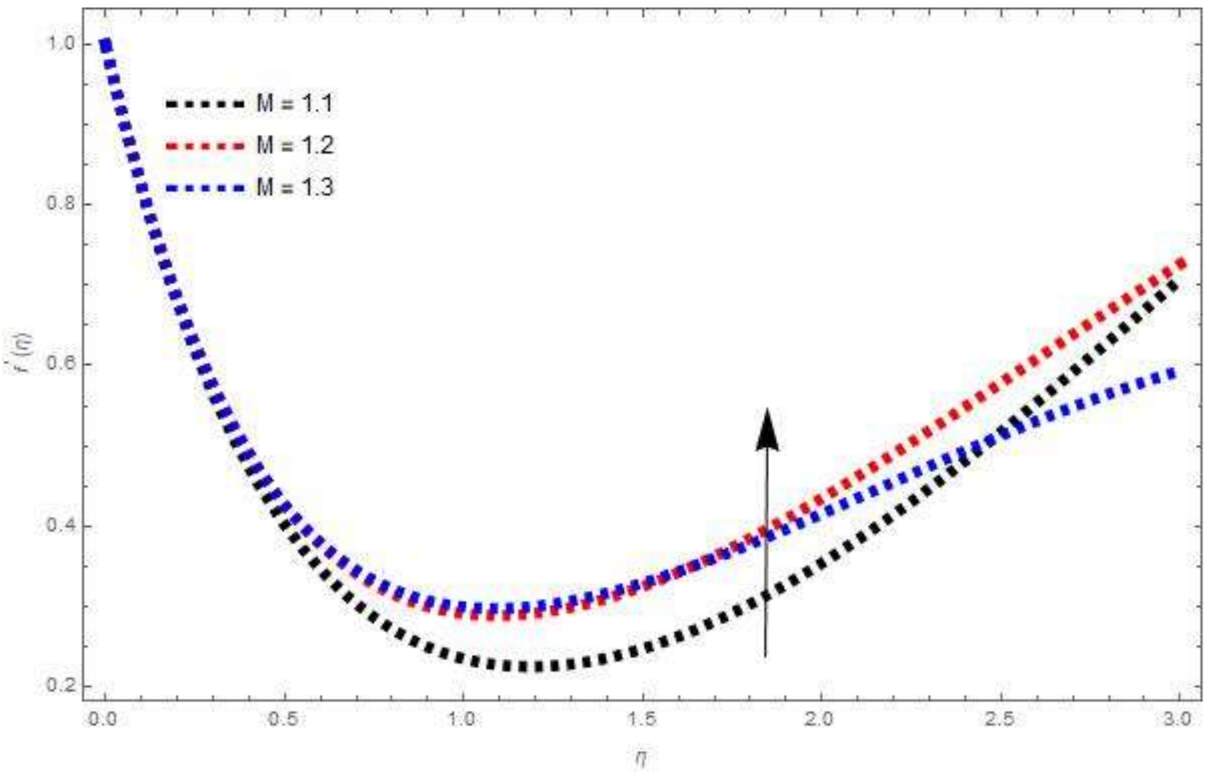

Fig. 4: M on $f'(\eta)$ without slip condition

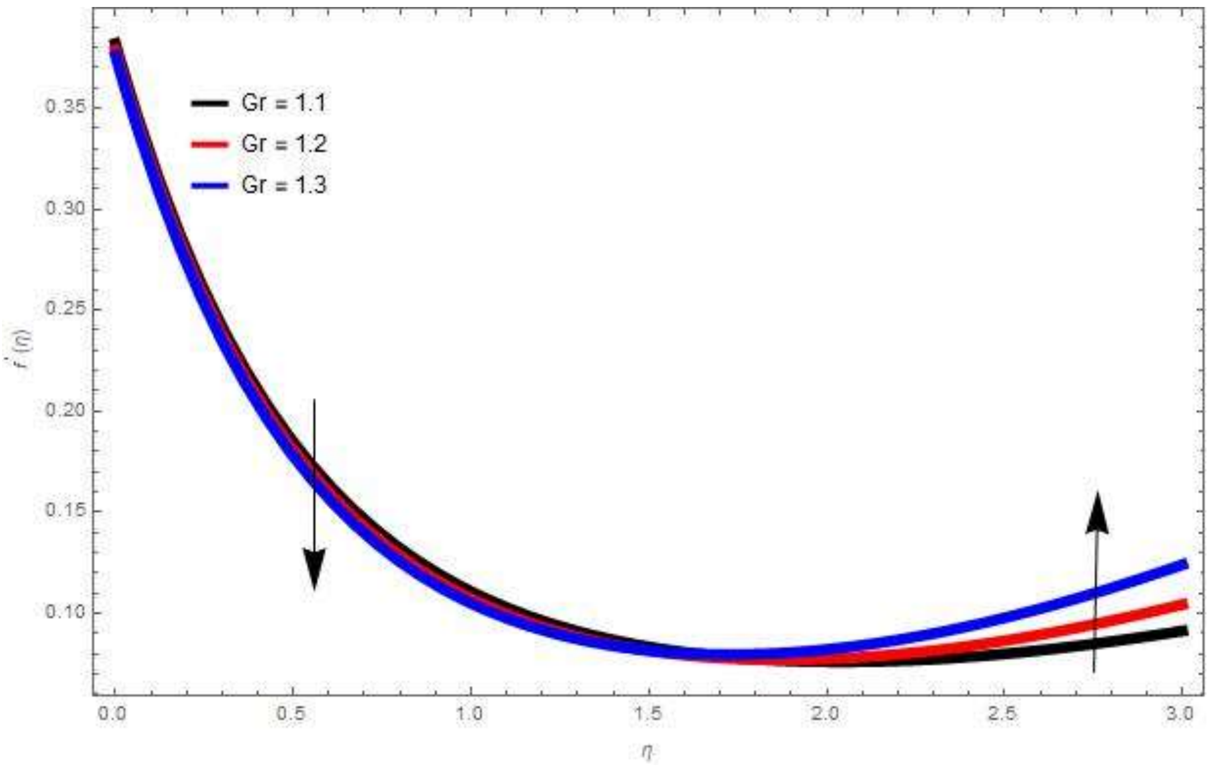

Fig. 5: Gr on $f'(\eta)$ with slip condition

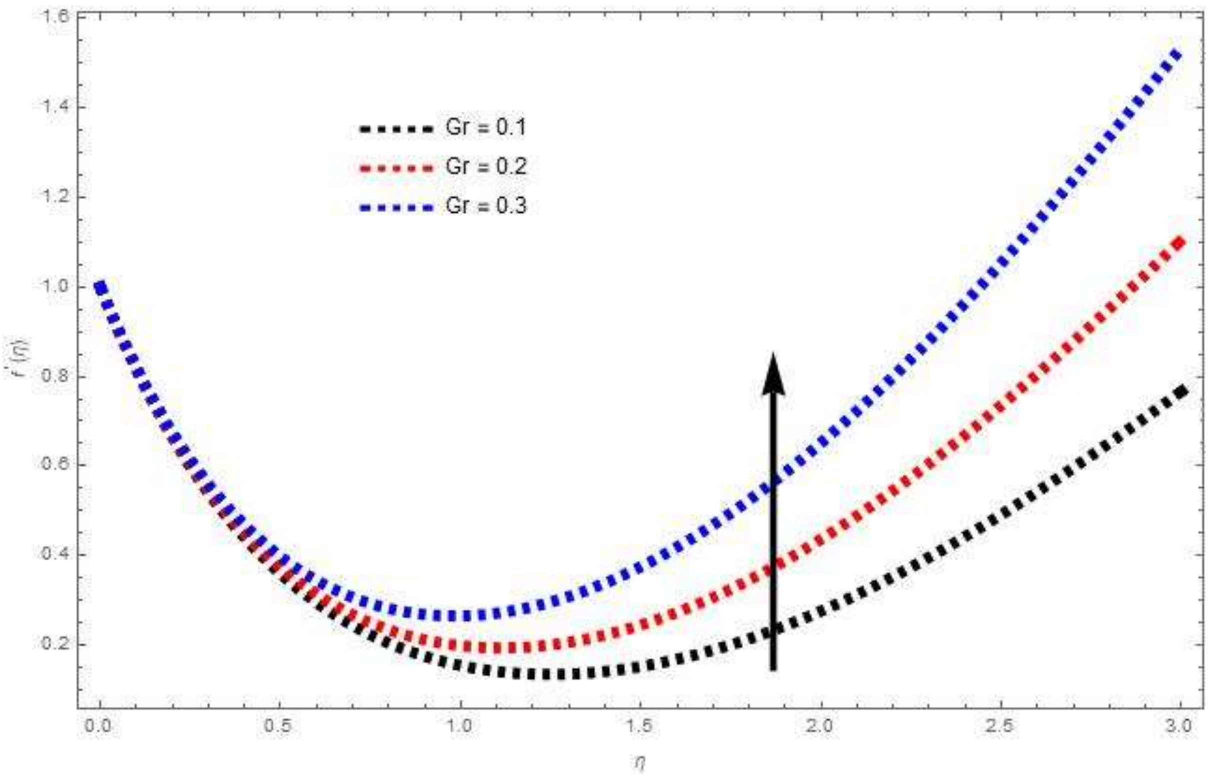

Fig. 6: Gr on $f'(\eta)$ without slip condition

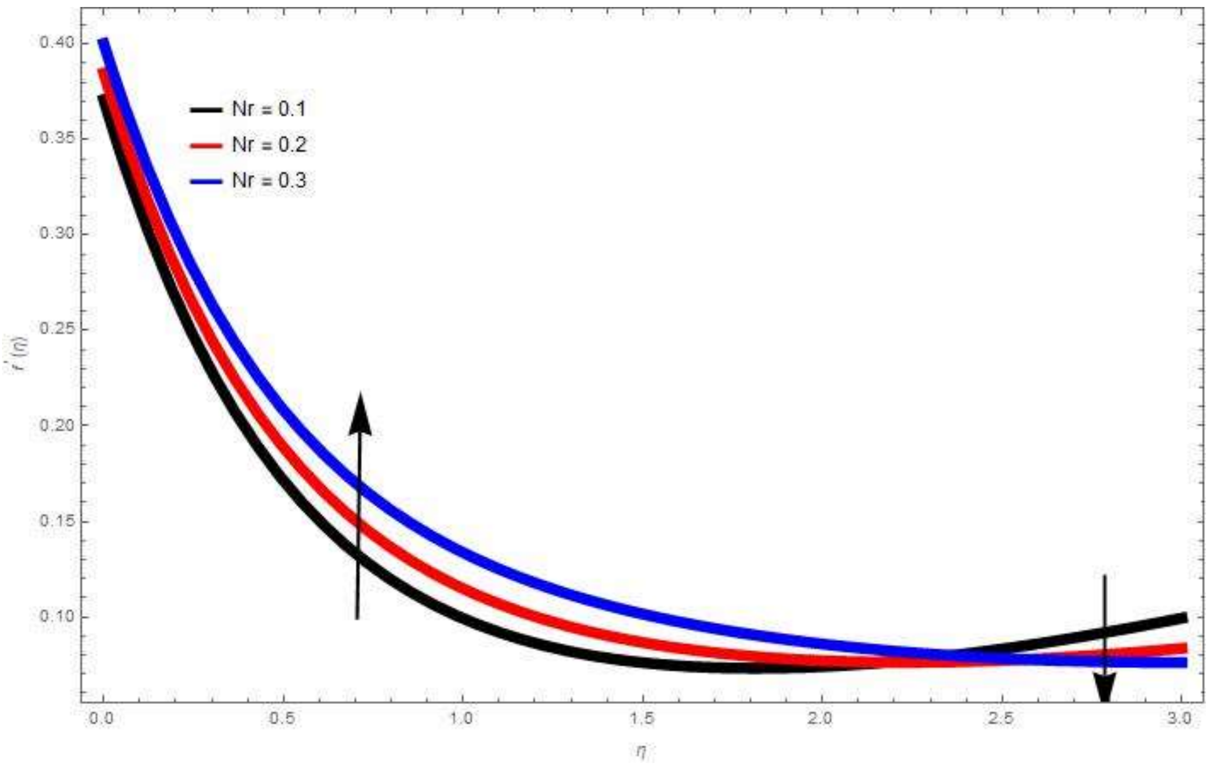

Fig. 7: Nr on $f'(\eta)$ with slip condition

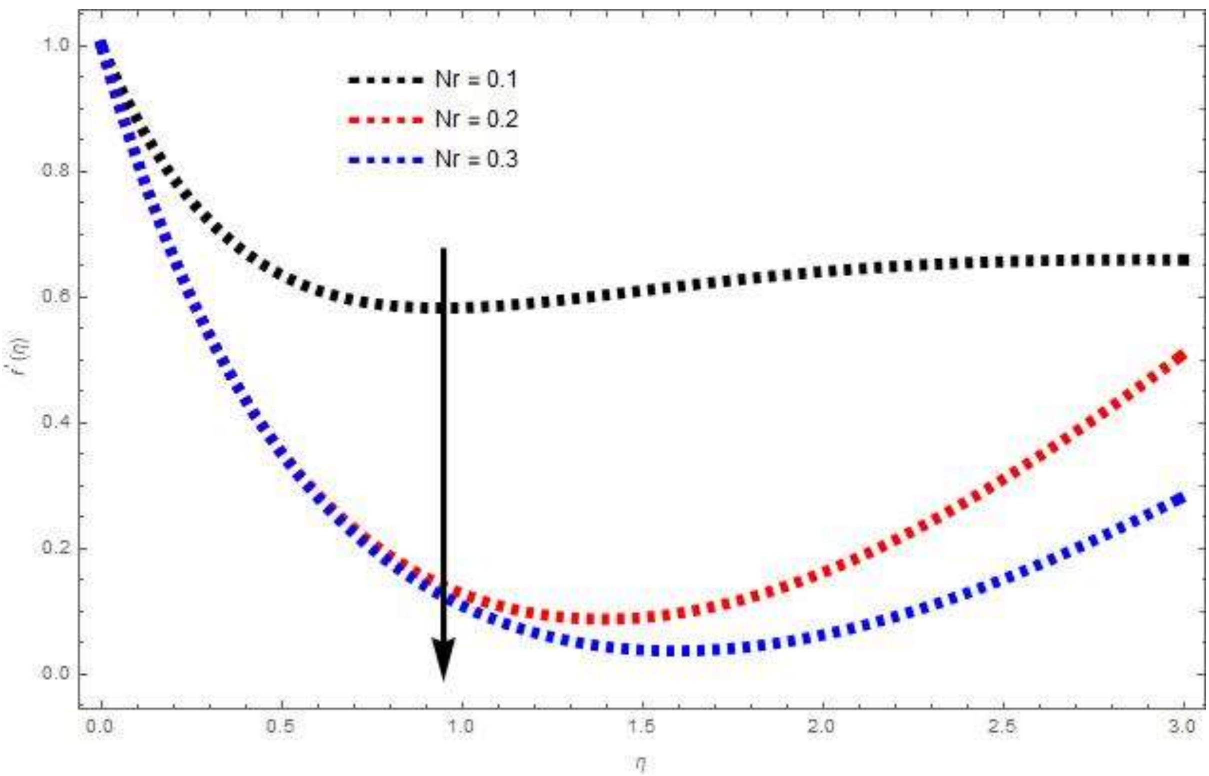

Fig. 8: Nr on $f'(\eta)$ without slip condition

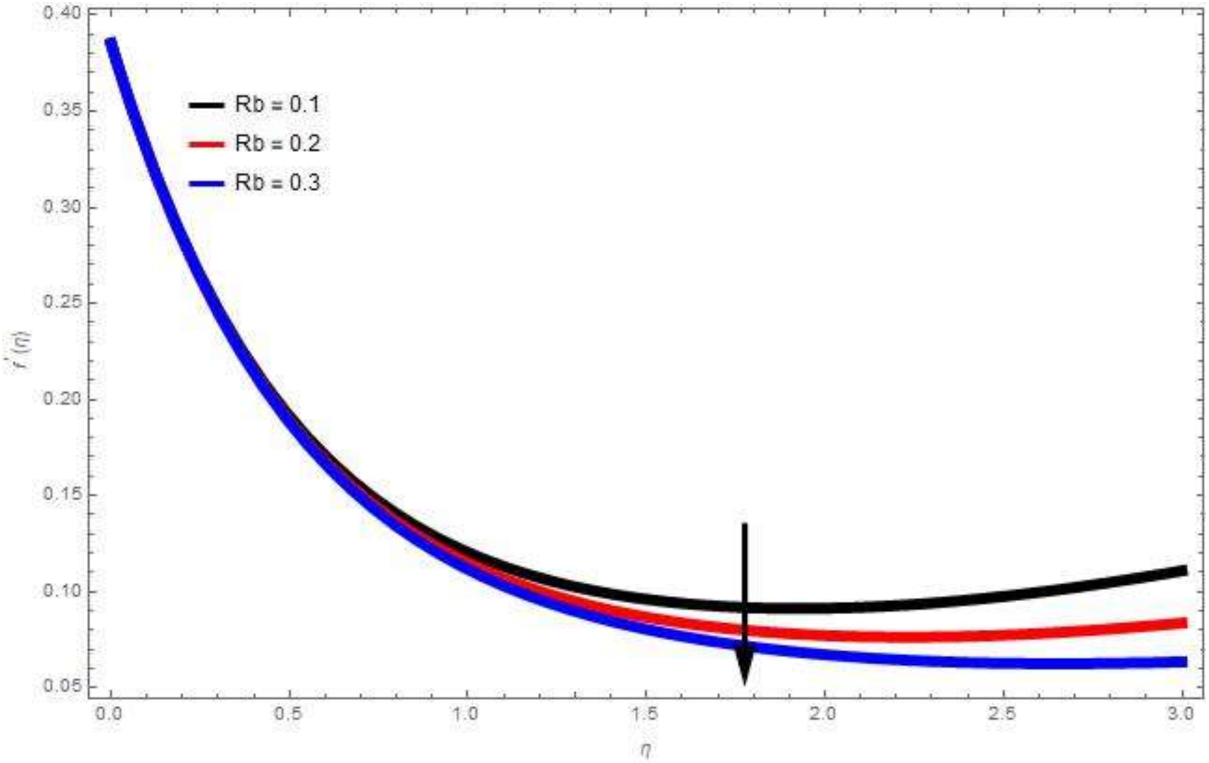

Fig. 9: Rb on $f'(\eta)$ with slip condition

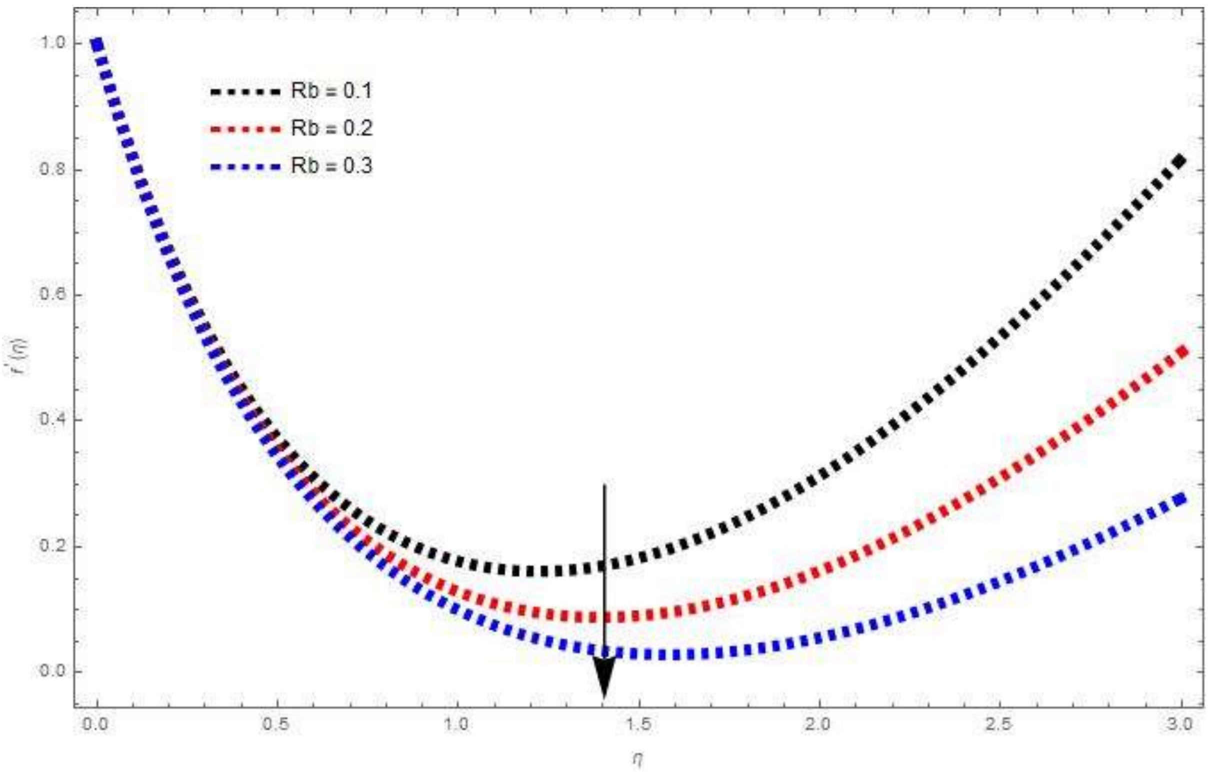

Fig. 10: Rb on $f'(\eta)$ without slip condition

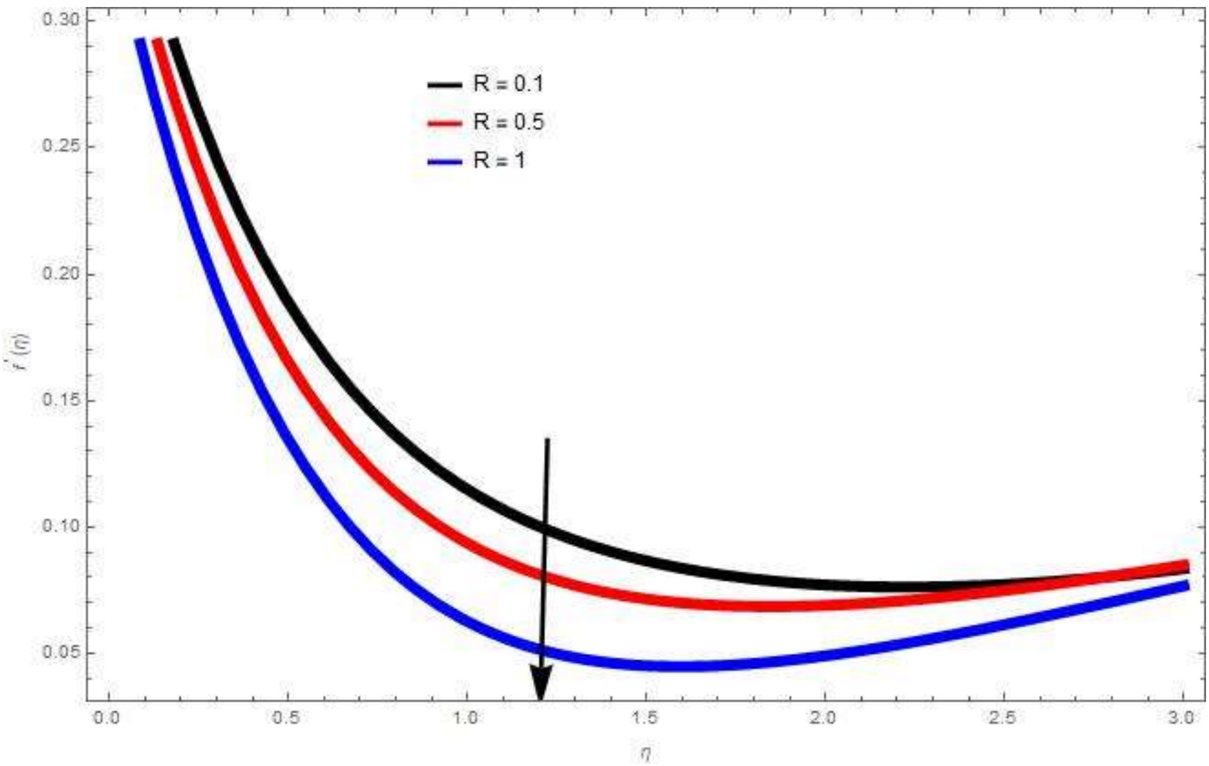

Fig. 11: R on $f'(\eta)$ with slip condition

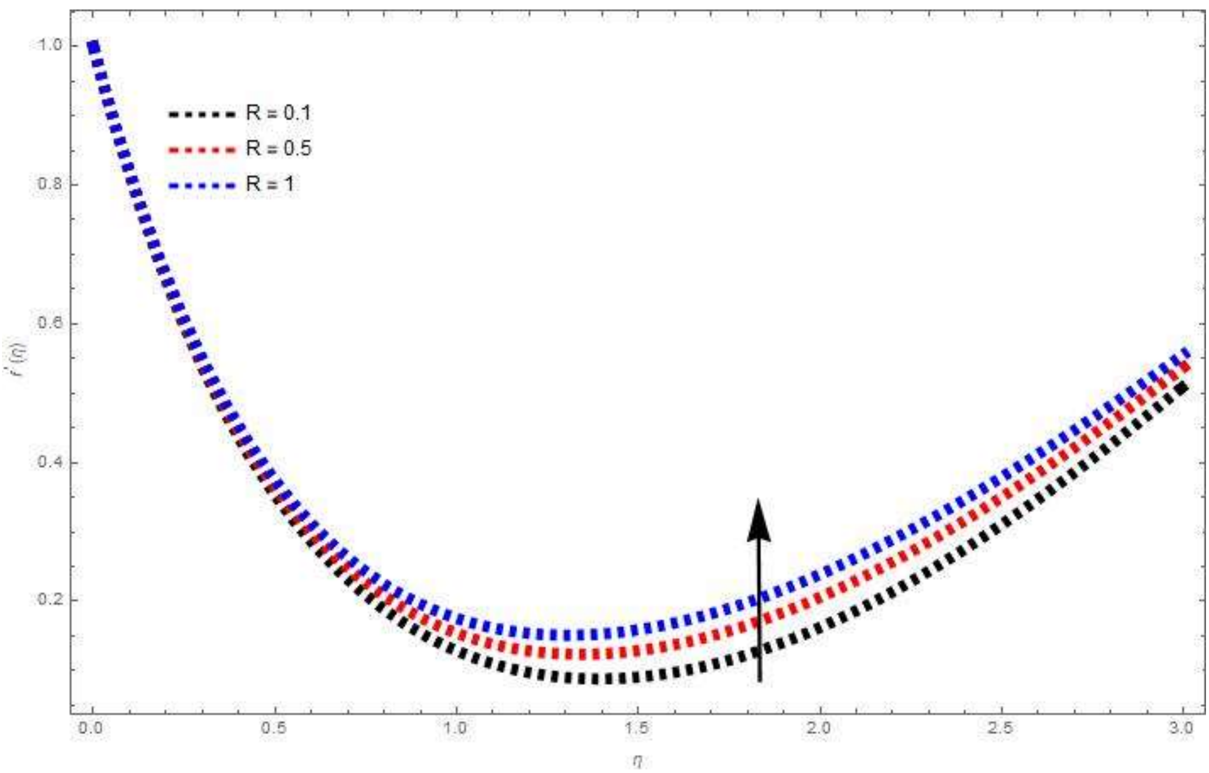

Fig. 12: R on $f'(\eta)$ without slip condition

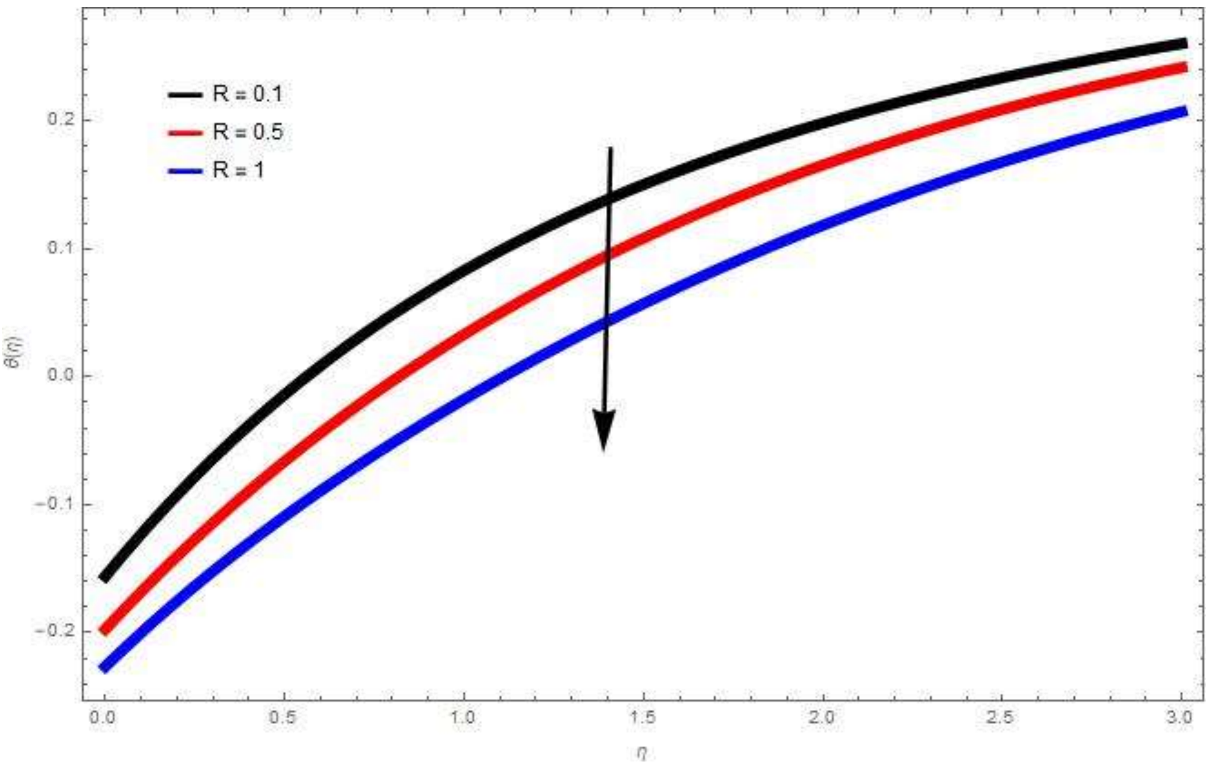

Fig. 13: R on $\theta(\eta)$ with slip condition

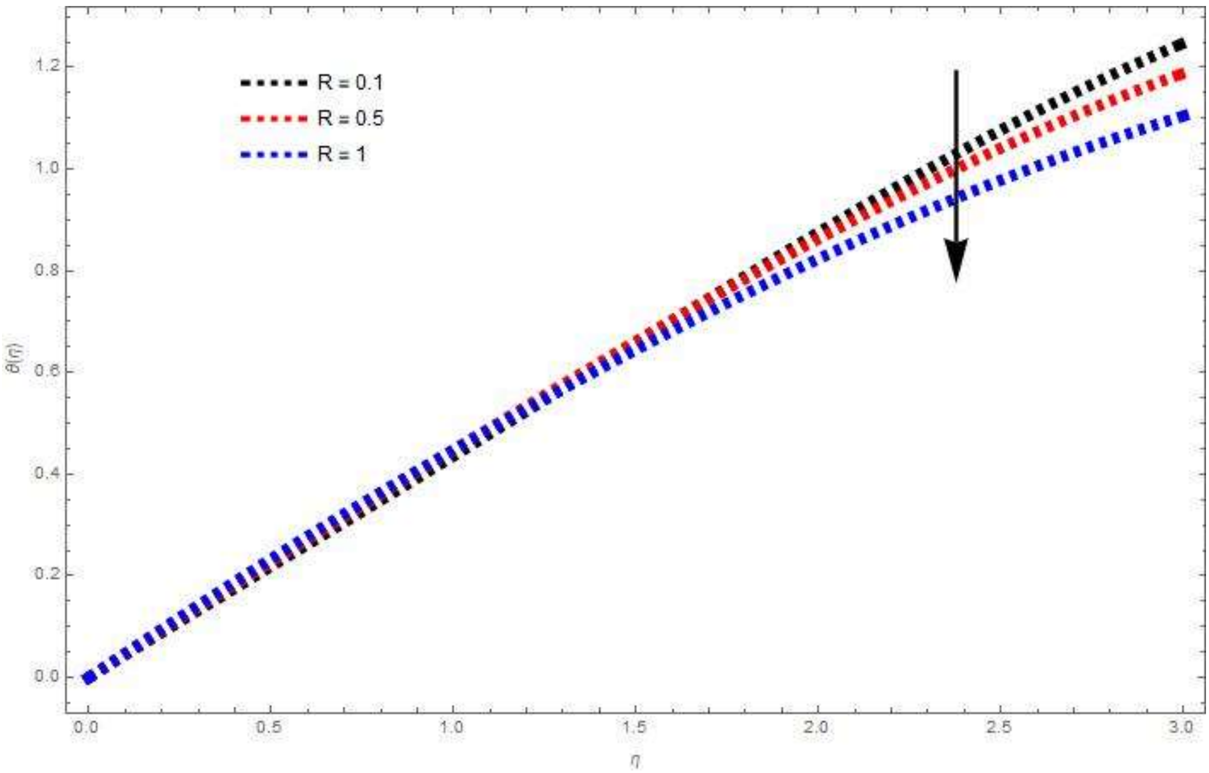

Fig. 14: R on $\theta(\eta)$ without slip condition

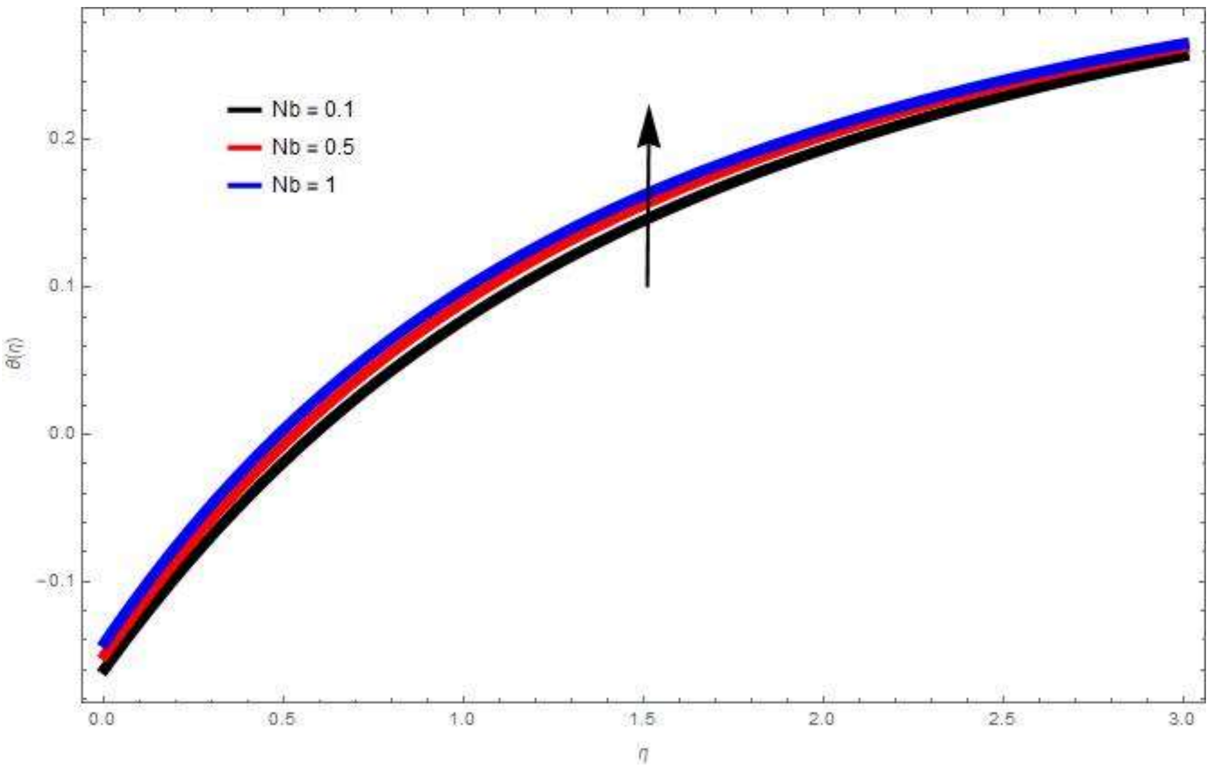

Fig. 15: Nb on $\theta(\eta)$ with slip condition

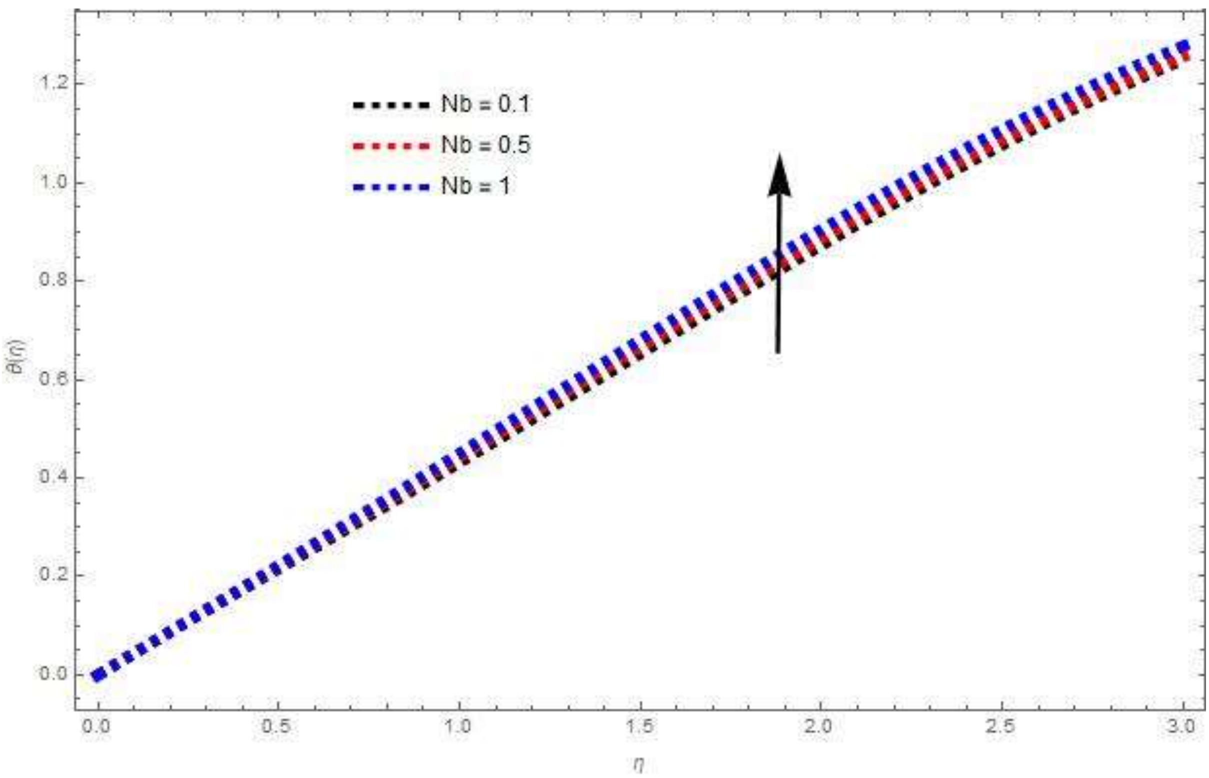

Fig. 16: Nb on $\theta(\eta)$ without slip condition

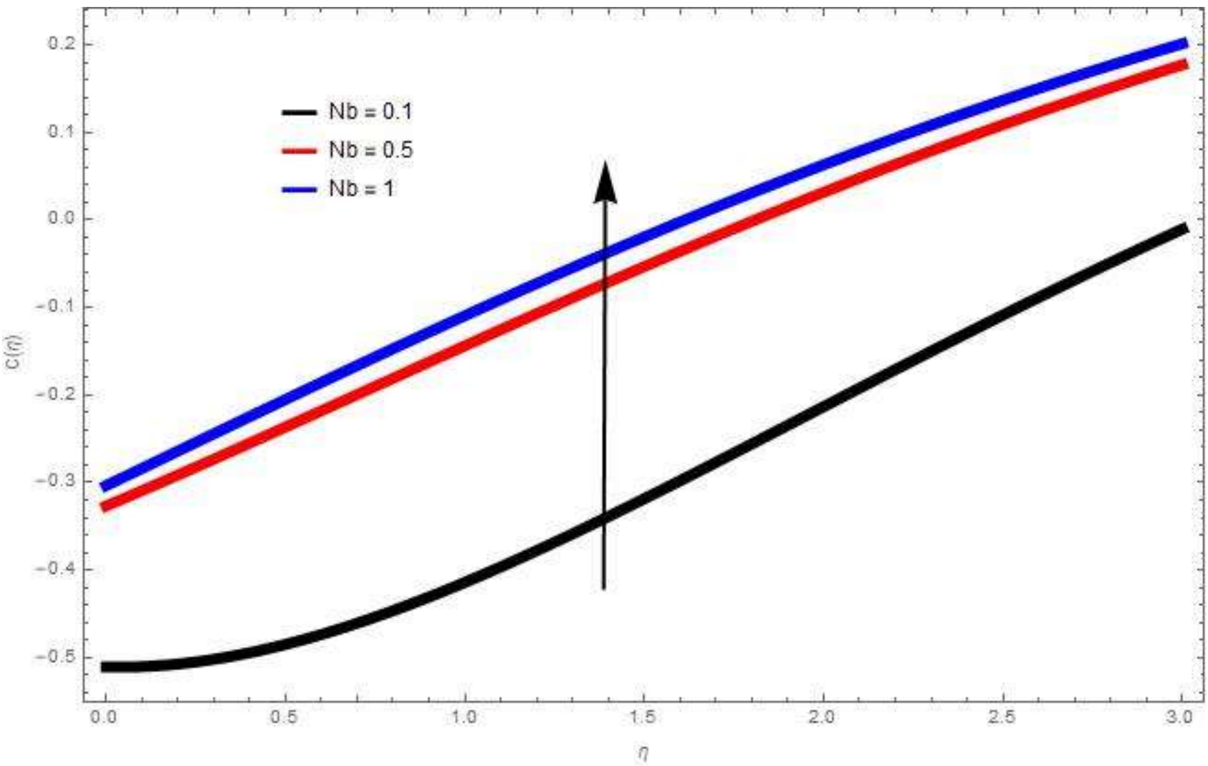

Fig. 17: Nb on $C(\eta)$ with slip condition

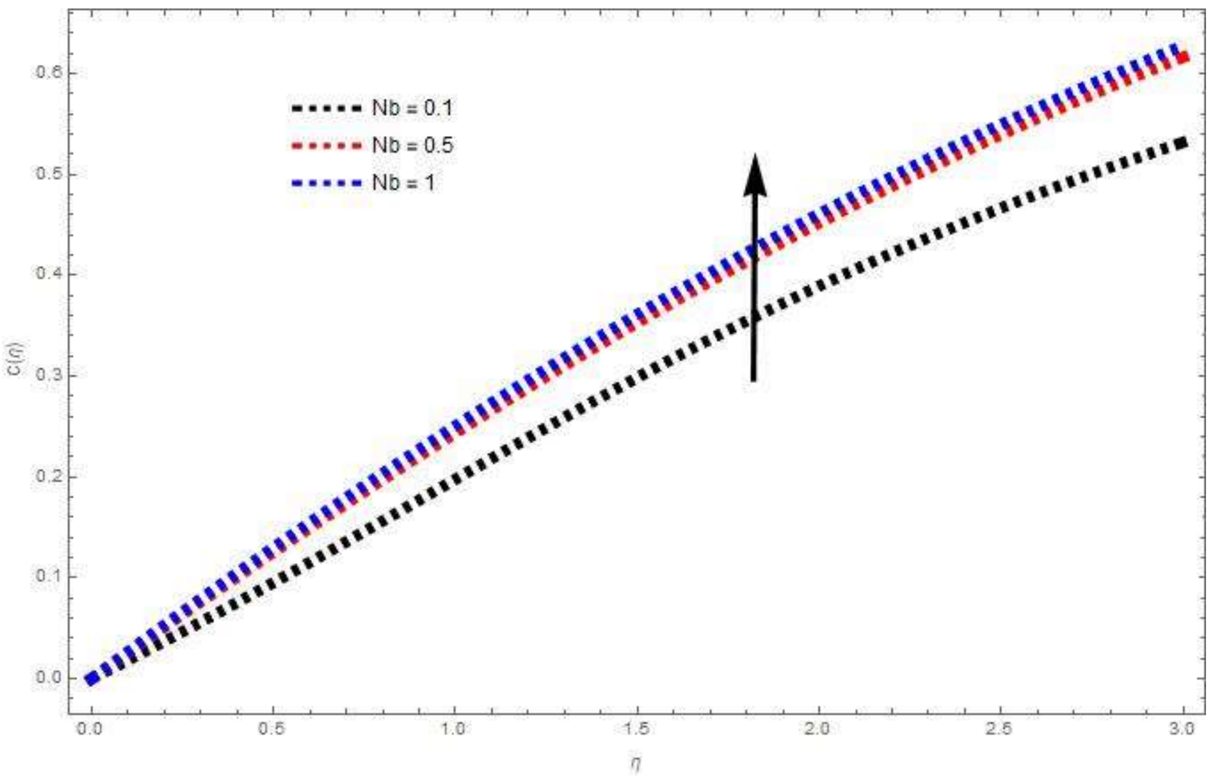

Fig. 18: Nb on $C(\eta)$ without slip condition

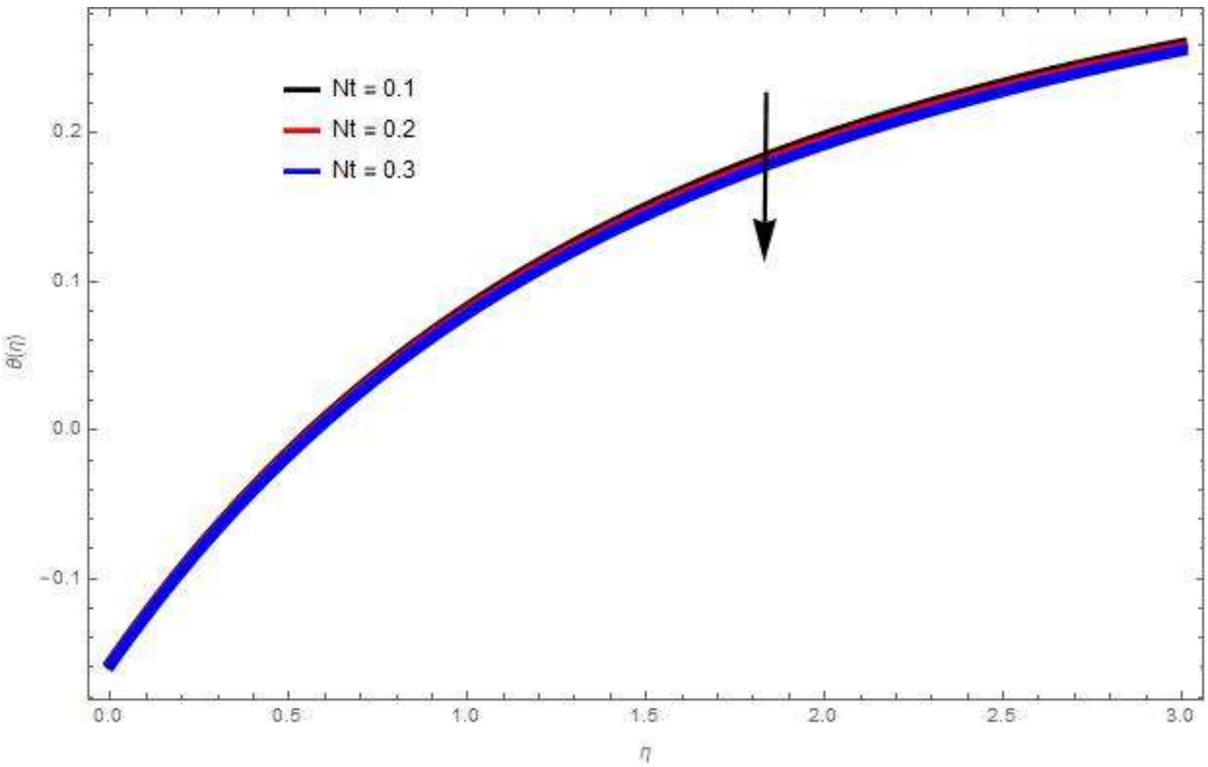

Fig. 19: Nt on $\theta(\eta)$ with slip condition

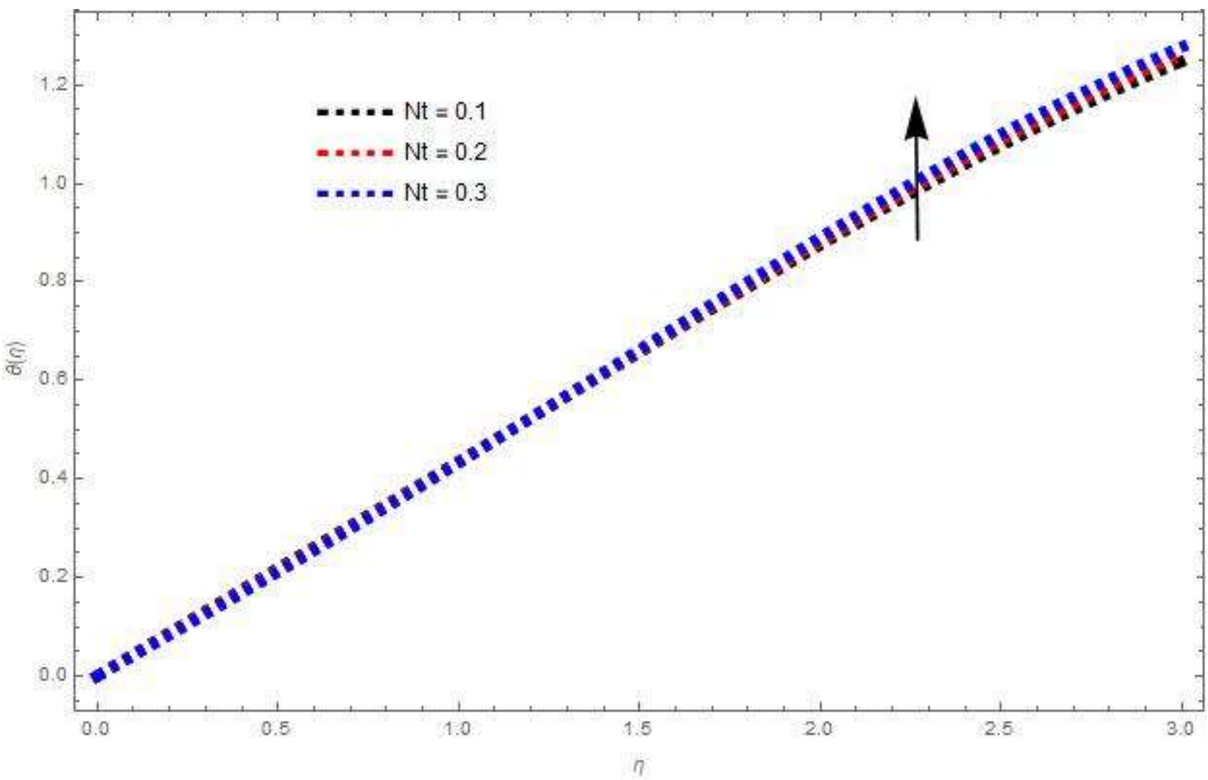

Fig. 20: Nt on $\theta(\eta)$ without slip condition

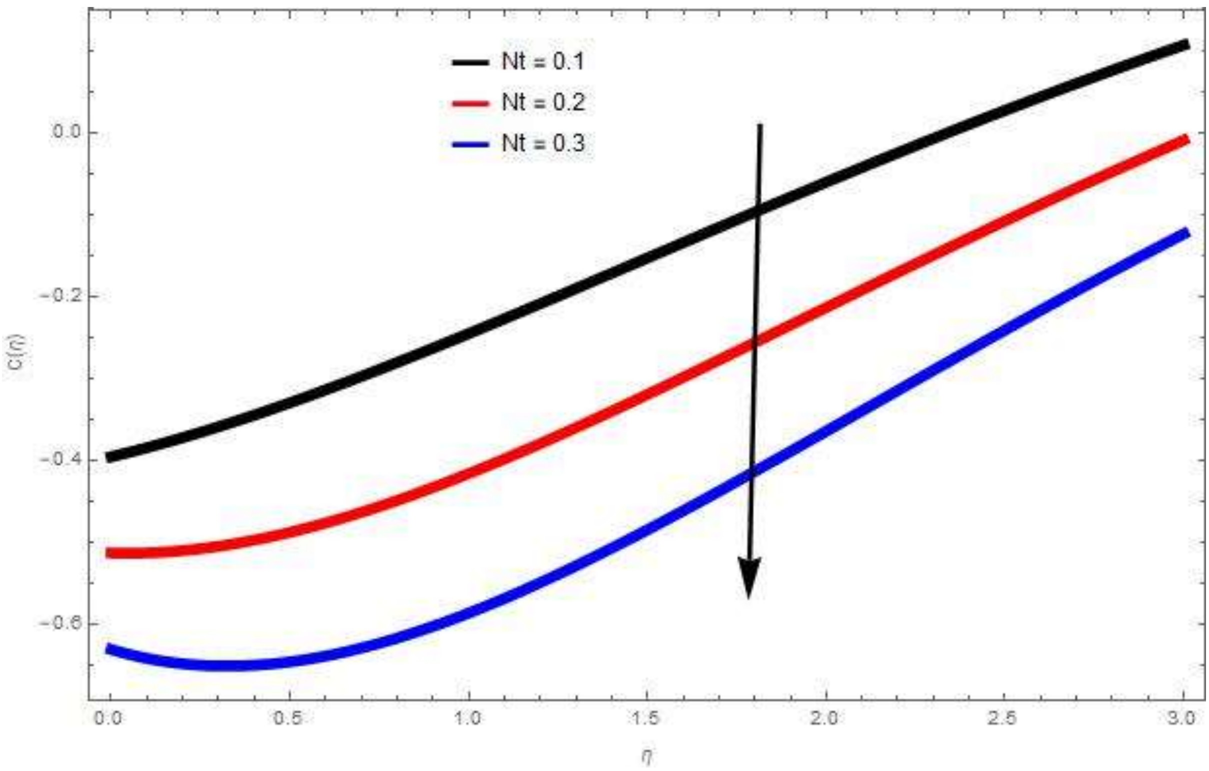

Fig. 21: Nt on $C(\eta)$ with slip condition

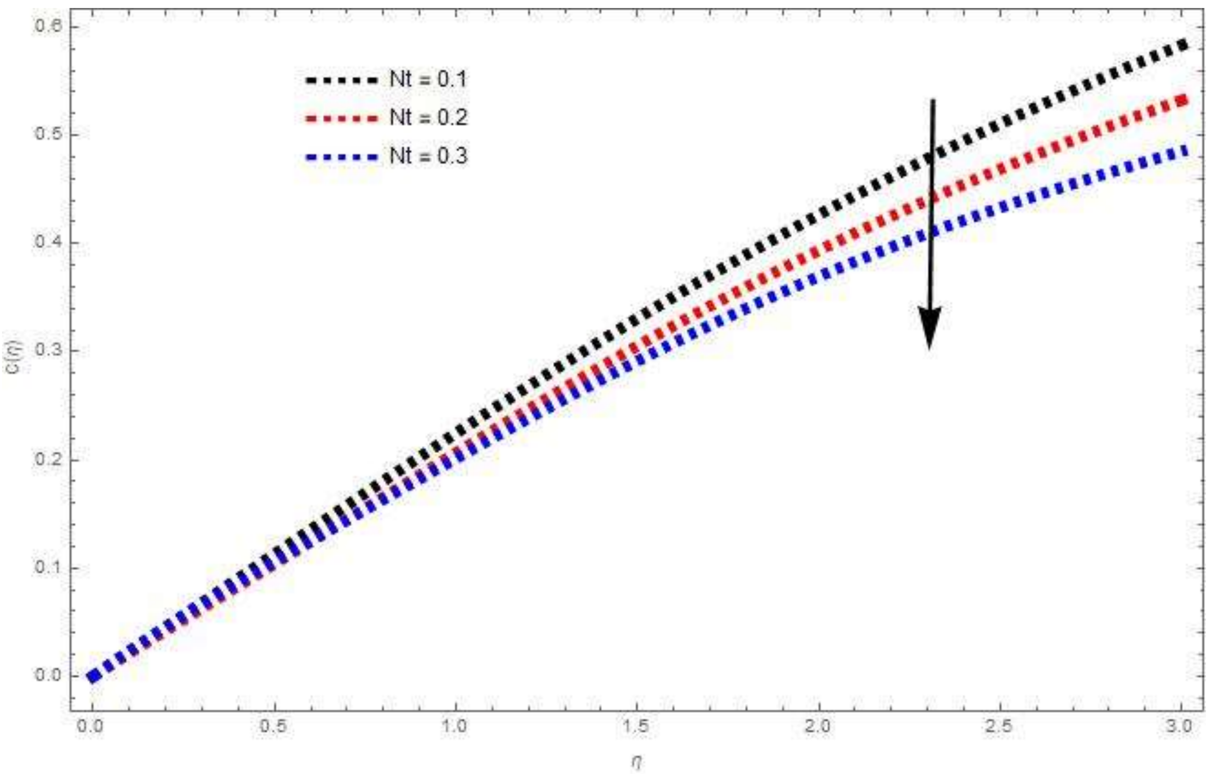

Fig. 22: Nt on $C(\eta)$ without slip condition

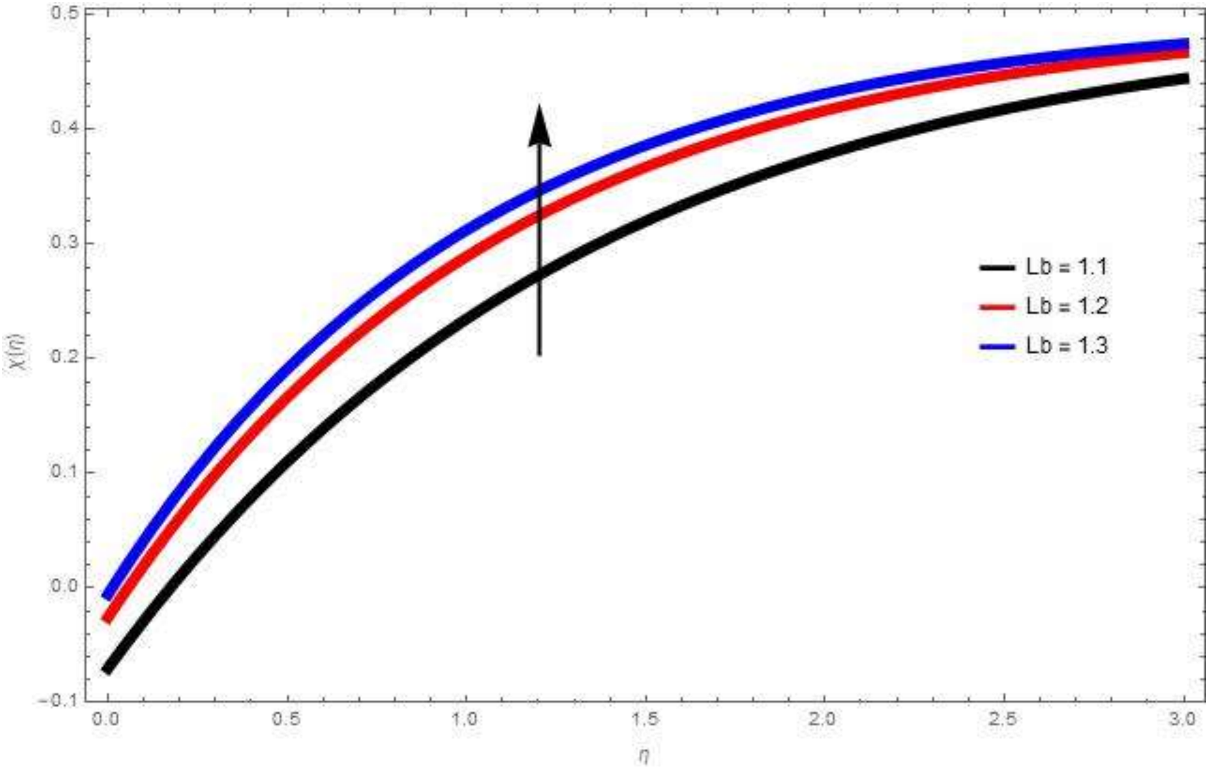

Fig. 23: Lb on $\chi(\eta)$ with slip condition

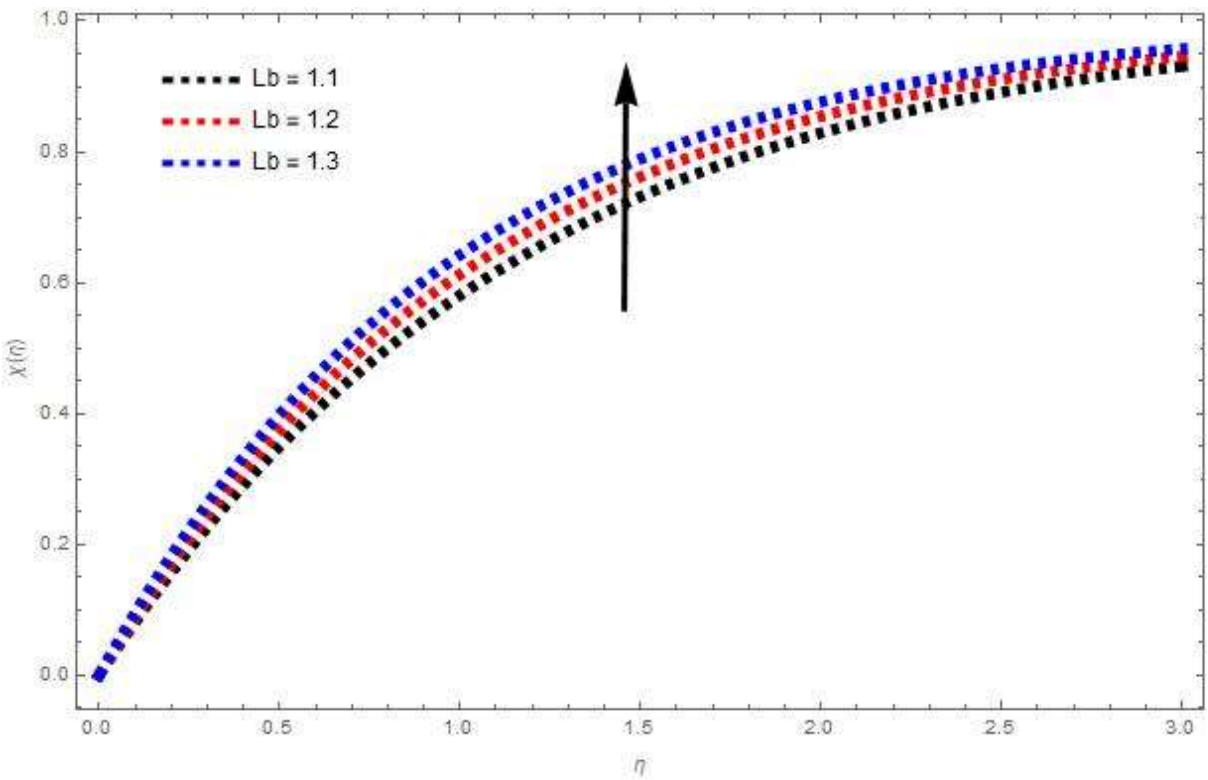

Fig. 24: Lb on $\chi(\eta)$ without slip condition

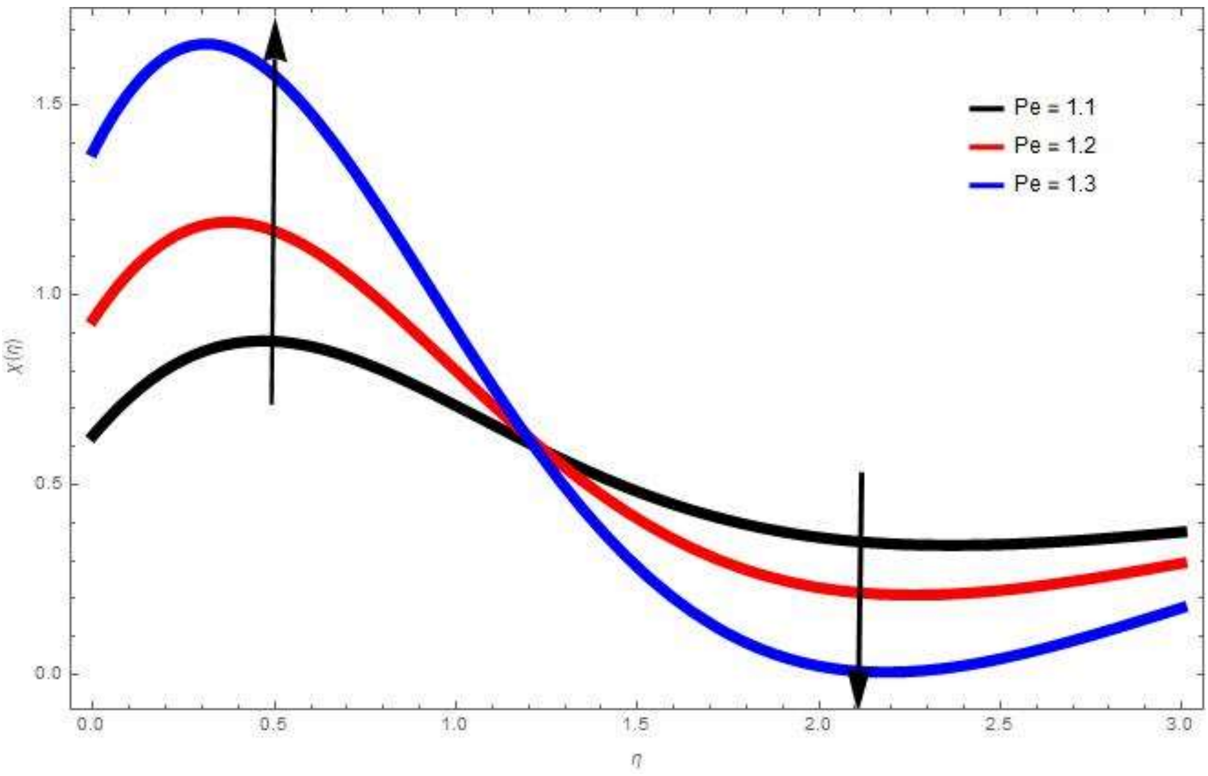

Fig. 25: Pe on $\chi(\eta)$ with slip condition

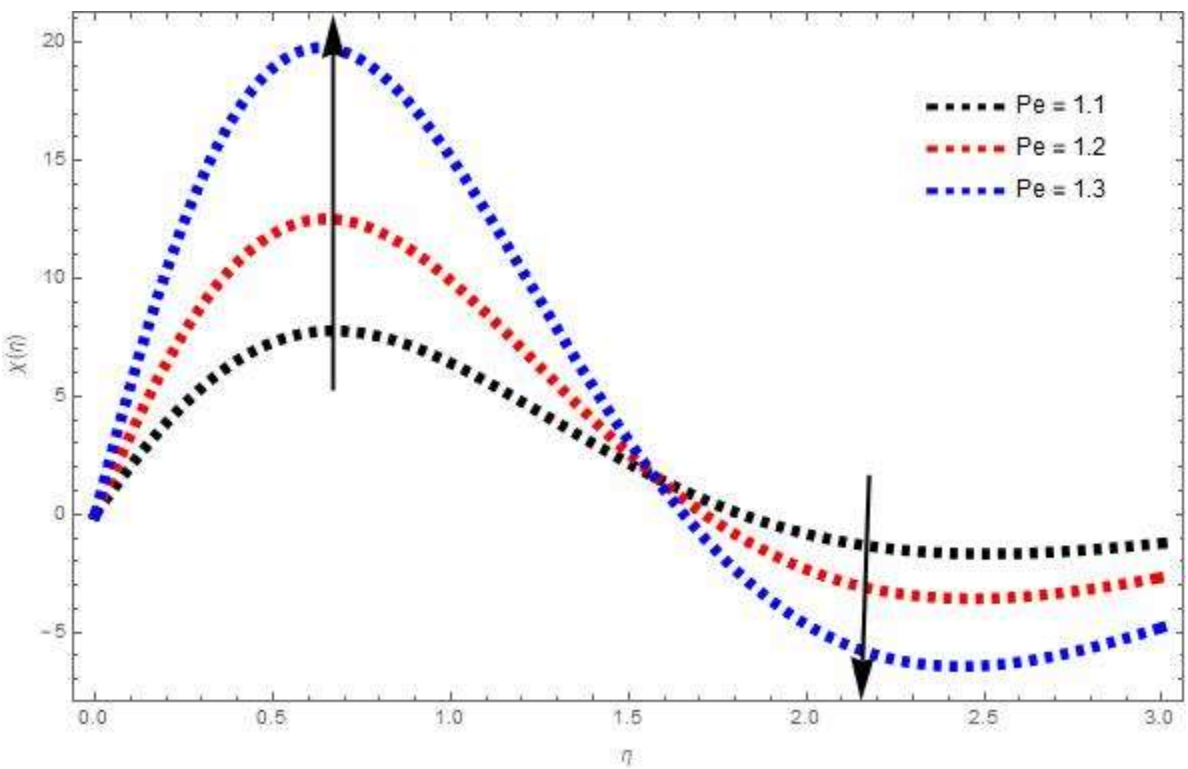

Fig. 26: Pe on $\chi(\eta)$ without slip condition

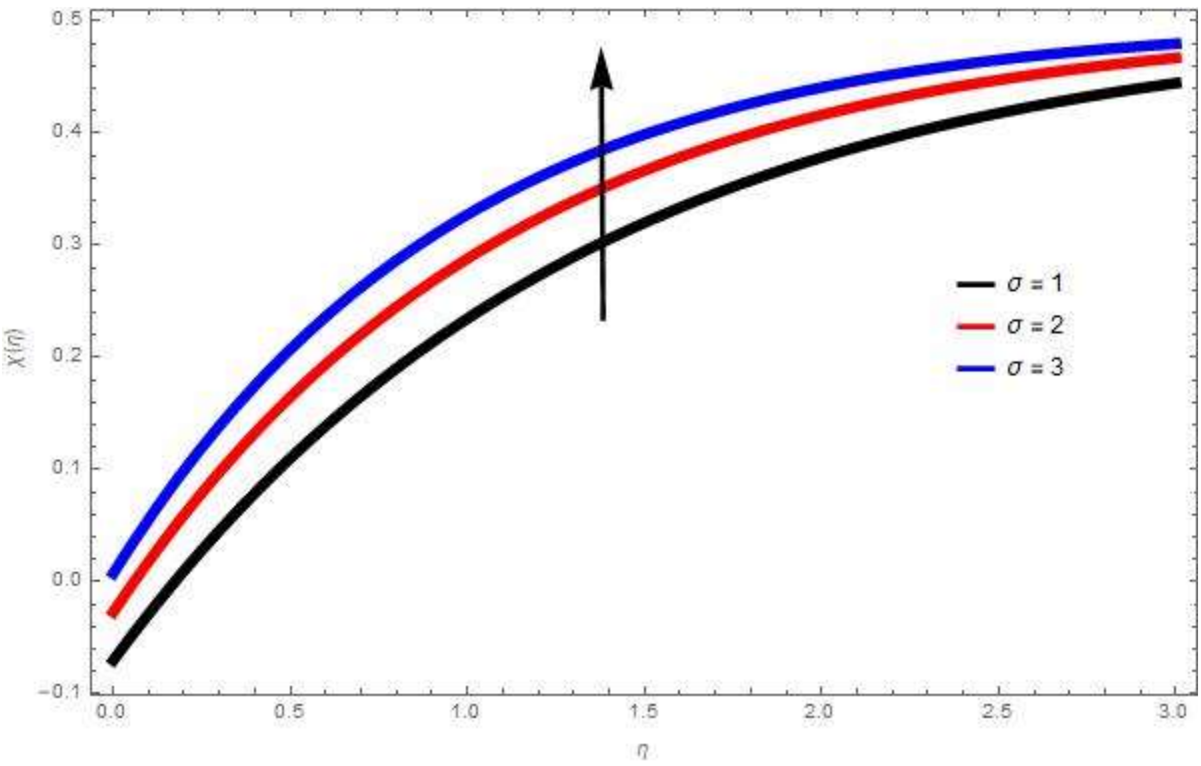

Fig. 27: σ on $\chi(\eta)$ with slip condition

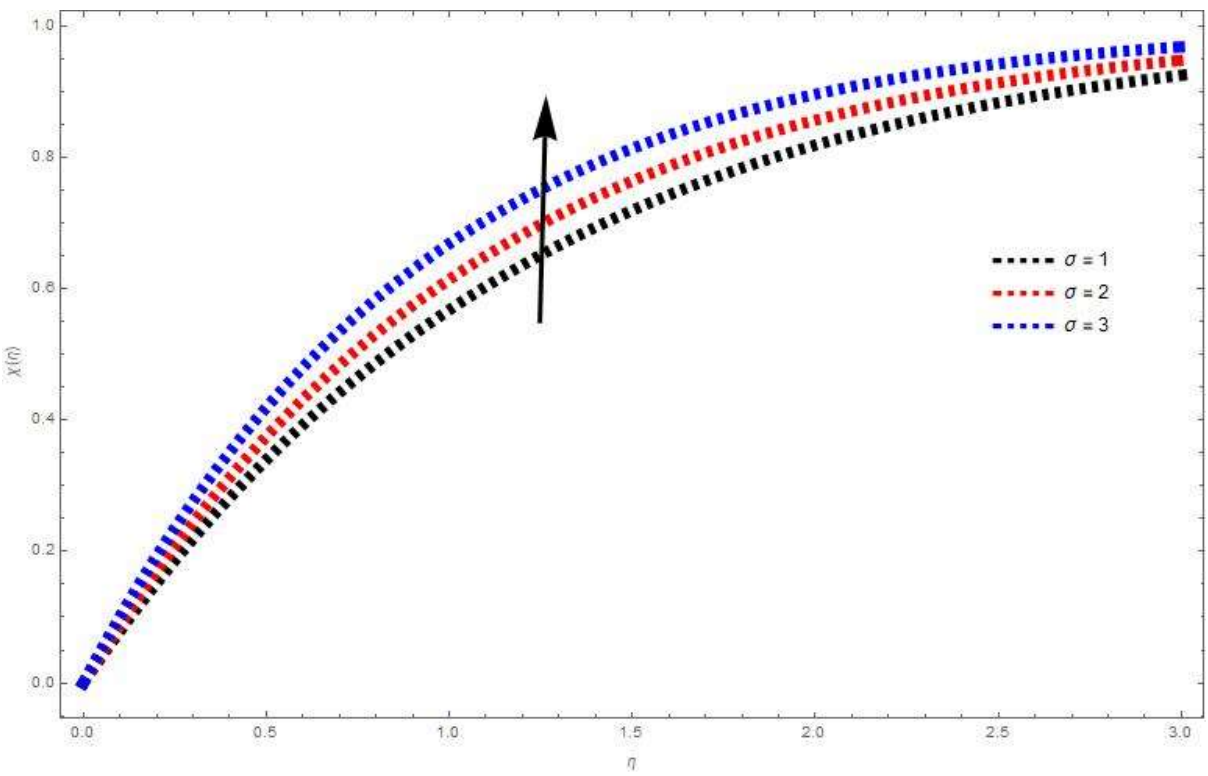

Fig. 28: σ on $\chi(\eta)$ without slip condition

Fig.2 represents the mixed h −curves for the velocity, temperature, concentration and zita profiles. Fig. 3 & 4 depict the effect of MHD parameter on velocity profile. From the figures it is clear that the fluid momentum retards as the value of MHD parameter rises. Fig.5 & 6 show the impact of thermal grashof number Gr on velocity profile. The Thermal Grashof number represents the relationship between the buoyancy force and the viscous hydrodynamic force. As the value of Gr increases, the buoyancy force also increases, leading to a subsequent rise in fluid velocity. This relationship is depicted in the figures, where an increase in Gr results in a higher fluid velocity. Fig. 7 & 8 indicate the effect of thermal radiation parameter Nr on velocity profile and it is observed that the velocity profile has the dual impact with the rise of Nr with slip condition but without slip condition the velocity decreases as Nr increases. The fluid momentum hindered with rise of Bio Convective Reyligh Rb number as seen in Figs. 9 & 10. In Fig. 11 the fluid motion hampered with the rise of radiation parameter R in slip condition while it has reverse impact without slip condition as seen in Fig.12. In Figs. 13 & 14 the heat transfer reduces as radiation parameter R soars. From Figs. 15 – 18 the temperature and concentration profiles rise with the rise of Brownian motion parameter Nb. In Fig. 19 the temperature reduces for the boosted values of Thermophoresis parameter Nt whereas in Fig.20 it has the reverse impact. Concentration declined with the rise of Thermophoresis parameter Nt as seen in Figs. 21 & 22. The impact of Lewis Number Lb on Micro Organism Profile $\chi(\eta)$ is shown in Fig.23 & 24 and they depict that Micro Organism enhanced with the boosted values of Lewis Number Lb. In Figs. 25 & 26 it is observed that Peclet number Pe has mixed impact on Micro Organism. The effect of electric conductivity parameter σ on Micro Organism profile is seen in Fig.27 & 28 and it shows that the Micro Organism profile enhanced with the rise of electric conductivity.

5. CONCLUSION

The study focused on the behavior of a two-dimensional Nanofluid in the presence of a magnetic field. The effects of various physical parameters such as chemical reaction, thermophoresis, gyrotactic micro motile organisms thermal radiation, and Brownian motion were taken into account. The dimensionless fluid flow governing equations were solved numerically using MATHEMATICA. The results obtained were presented graphically for both slip and non-slip conditions. Some of the key findings are as follows:

• The fluid momentum f' exhibits positive behavior for increased values of M, Gr and Nr, and negative behavior for increased values of Rb and R.

• The heat transfer of the nanofluid is raised for higher values of Nb, and exhibits a decreasing behavior for higher values of Nt and R.

• The concentration of the nanofluid increases for higher values of Nb, and shows the opposite behavior for Nt.

• The profile of the micro motile organism increases for higher values of Pe, Lb, and σ.

References:

[1] Choi, S.U.S. “Enhancing Thermal Conductivity of Fluids with Nanoparticles.” *ASME International Mechanical Engineering Congress and Exposition*, vol. 231, 1995, pp. 99–105.

[2] Eastman, J.A., et al. “Novel Thermal Properties of Nanostructured Materials.” *J. Metastable Nanocryst Mater*, vol. 2, 1999, pp. 629–637.

[3] Imran Ullah, Sharidan Shafie, Ilyas Khan, Kai Long Hsiao, Brownian diffusion and thermophoresis mechanisms in Casson fluid over a moving wedge, Results in Physics, Volume 9, 2018, Pages 183-194, ISSN 2211-3797, https://doi.org/10.1016/j.rinp.2018.02.021.

[4] M. Sheikholeslami, M.M. Rashidi, Dhafer M. Al Saad, F. Firouzi, Houman B. Rokni, G. Domairry, Steady nanofluid flow between parallel plates considering thermophoresis and Brownian effects, Journal of King Saud University - Science, Volume 28, Issue 4, 2016, Pages 380-389, ISSN 1018-3647, https://doi.org/10.1016/j.jksus.2015.06

[5] Tasawar Hayat, Sajid Qayyum, Ahmed Alsaedi, Anum Shafiq, Theoretical aspects of Brownian motion and thermophoresis on nonlinear convective flow of magneto Carreau nanofluid with Newtonian conditions, Results in Physics, Volume 10, 2018, Pages 521-528, ISSN 2211-3797, https://doi.org/10.1016/j.rinp.2018.04.027.

[6] Habib-Olah Sayehvand, Amir Basiri Parsa, A new numerical method for investigation of thermophoresis and Brownian motion effects on MHD nanofluid flow and heat transfer between parallel plates partially filled with a porous medium, Results in Physics, Volume 7, 2017, Pages 1595-1607, ISSN 2211-3797, https://doi.org/10.1016/j.rinp.2017.02.004.

[7] Hartmann, J., and F. Lazarus. “Theory of Laminar Flow of Electrically Conductive Liquids in a Homogeneous Magnetic Field.” *15th International Congress of Refrigeration*, 1937.

[8] M. Jayachandra Babu, N. Sandeep, S. Saleem, Free convective MHD Cattaneo-Christov flow over three different geometries with thermophoresis and Brownian motion, Alexandria Engineering Journal, Volume 56, Issue 4, 2017, Pages 659-669, ISSN 1110-0168, https://doi.org/10.1016/j.aej.2017.01.005.

[9] F. Mabood, S.M. Ibrahim, W.A. Khan, Framing the features of Brownian motion and thermophoresis on radiative nanofluid flow past a rotating stretching sheet with magnetohydrodynamics, Results in Physics, Volume 6, 2016, Pages 1015-1023, ISSN 2211-3797, https://doi.org/10.1016/j.rinp.2016.11.046.

[10] Hari R. Kataria, Akhil S. Mittal, Mathematical model for velocity and temperature of gravity-driven convective optically thick nanofluid flow past an oscillating vertical plate in presence of magnetic field and radiation, Journal of the Nigerian Mathematical Society, Volume 34, Issue 3, 2015, Pages 303-317, ISSN 0189-8965, https://doi.org/10.1016/j.jnnms.2015

[11] M. Sheikholeslami, Hari R. Kataria, Akhil S. Mittal, Effect of thermal diffusion and heat-generation on MHD nanofluid flow past an oscillating vertical plate through porous medium, Journal of Molecular Liquids, Volume 257, 2018, Pages 12-25, ISSN 0167-7322, https://doi.org/10.1016/j.molliq.2018.02.079.

[12] Harshad R Patel, Snehal D Patel, Rakesh Darji, Mathematical Study of unsteady micropolar fluid flow due to non-linear stretched sheet in the presence of magnetic field, International Journal of Thermofluids, Volume 16, 2022, 100232, ISSN 2666-2027, https://doi.org/10.1016/j.ijft.2022.100232.

[13] Hari R. Kataria, Harshad R. Patel, Effect of thermo-diffusion and parabolic motion on MHD second grade fluid flow with ramped wall temperature and ramped surface

concentration, Alexandria Engineering Journal, Volume 57, Issue 1, 2018, Pages 73-85, ISSN 1110-0168, https://doi.org/10.1016/j.aej.2016.11.014.

[14] S. Rosseland, Astrophysik und atom-theoretische Grundlagen, Springer-Verlag, Berlin, 1931.

[15] C. Sulochana, G.P. Ashwinkumar, N. Sandeep, Transpiration effect on stagnation-point flow of a Carreau nanofluid in the presence of thermophoresis and Brownian motion, Alexandria Engineering Journal, Volume 55, Issue 2, 2016, Pages 1151-1157, ISSN 1110-0168, https://doi.org/10.1016/j.aej.2016.03.031.

[16] Iskandar Waini, Khairum Bin Hamzah, Najiyah Safwa Khashi'ie, Nurul Amira Zainal, Abdul Rahman Mohd Kasim, Anuar Ishak, Ioan Pop, Brownian and thermophoresis diffusion effects on magnetohydrodynamic Reiner–Philippoff nanofluid flow past a shrinking sheet, Alexandria Engineering Journal, Volume 67, 2023, Pages 183-192, ISSN 1110-0168, https://doi.org/10.1016/j.aej.2022.12.056.

[17] G. Kalpana, K.R. Madhura, Ramesh B. Kudenatti, Magnetohydrodynamic boundary layer flow of hybrid nanofluid with the thermophoresis and Brownian motion in an irregular channel: A numerical approach, Engineering Science and Technology, an International Journal, Volume 32, 2022, 101075, ISSN 2215-0986, https://doi.org/10.1016/j.jestch.2021.11.001.

[18] M. Hatami, S.E. Ghasemi, Thermophoresis and Brownian diffusion of nanoparticles around a vertical cone in a porous media by Galerkin finite element method (GFEM), Case Studies in Thermal Engineering, Volume 28, 2021, 101627, ISSN 2214-157X, https://doi.org/10.1016/j.csite.2021.101627.

[19] Jagadish V. Tawade, C.N. Guled, Samad Noeiaghdam, Unai Fernandez-Gamiz, Vediyappan Govindan, Sundarappan Balamuralitharan, Effects of thermophoresis and Brownian motion for thermal and chemically reacting Casson nanofluid flow over a linearly stretching sheet, Results in Engineering, Volume 15, 2022, 100448, ISSN 2590-1230, https://doi.org/10.1016/j.rineng.2022.100448.

[20] Shahzad Ahmad, Anique Ahmad, Kashif Ali, Hina Bashir, Muhammad Farooq Iqbal,Effect of non-Newtonian flow due to thermally-dependent properties over an inclined surface in the presence of chemical reaction, Brownian motion and thermophoresis, Alexandria Engineering Journal, Volume 60, Issue 5, 2021, Pages 4931-4945, ISSN 1110-0168, https://doi.org/10.1016/j.aej.2021.03.014.

[21] Yan Cao, Hamdi Ayed, Fahd Jarad, Hussein Togun, Hajar Alias, Alibek Issakhov, Mahidzal Dahari, Makatar Wae-hayee, Mohamed Hechmi El Ouni, MHD natural convection nanofluid flow in a heat exchanger: Effects of Brownian motion and thermophoresis for nanoparticles distribution, Case Studies in Thermal Engineering, Volume 28, 2021, 101394, ISSN 2214-157X, https://doi.org/10.1016/j.csite.2021.101394.

[22] Mehdi Bahiraei, Impact of thermophoresis on nanoparticle distribution in nanofluids, Results in Physics, Volume 7, 2017, Pages 136-138, ISSN 2211-3797, https://doi.org/10.1016/j.rinp.2016.12.012.

[23] Akhil S. Mittal, Hari R. Kataria, three dimensional CuO–Water nanofluid flow considering Brownian motion in presence of radiation, Karbala International Journal of Modern Science, Volume 4, Issue 3, 2018, Pages 275-286, ISSN 2405-609X, https://doi.org/10.1016/j.kijoms.2018.05.002.

[24] S Rosseland. Springer-verlag; berlin: 1931. Astrophysik und atom-theoretische Grundlagen

[25] Shijun Liao. Beyond perturbation: introduction to the homotopy analysis method. Chapman and Hall/CRC, 2003.

[26] N. Begum, S. Siddiqa, M. Hossain, Nanofluid bioconvection with variable thermophysical properties. J. Mol. Liquids 231 (2017) 325–332.

[27] D. Pal and S. K. Mondal, Magneto-bioconvection of Powell Eyring nanofluid over a permeable vertical stretching sheet due to gyrotactic microorganisms in the presence of nonlinear thermal radiation and Joule heating. Int. J. Ambient Energy 43 (1) (2022), 924–935.

[28] B. Ahmad, M. O. Ahmad, M. Farman, A. Akgül, M. B. Riaz, A significance of multi slip condition for inclined MHD nano-fluid flow with nonlinear thermal radiations, Dufuor and Sorrot, and chemically reactive bio-convection effect, South African Journal of Chemical Engineering 43 (2023) 135–145.